A PHYSICAL MODEL STUDY ON REINFORCEMENT OF A BREAKWATER CONSISTING OF TETRAPOD ARTIFICIAL BLOCKS

A THESIS SUBMITTED TO
THE GRADUATE SCHOOL OF NATURAL AND APPLIED SCIENCES
OF
MIDDLE EAST TECHNICAL UNIVERSITY

BY

BERKAY AKYOL

IN PARTIAL FULFILLMENT OF THE REQUIREMENTS
FOR
THE DEGREE OF MASTER OF SCIENCE
IN
CIVIL ENGINEERING

AUGUST 2022

Approval of the thesis:

A PHYSICAL MODEL STUDY ON REINFORCEMENT OF A BREAKWATER CONSISTING OF TETRAPOD ARTIFICIAL BLOCKS

submitted by **BERKAY AKYOL** in partial fulfillment of the requirements for the degree of **Master of Science** i**n Civil Engineering, Middle East Technical University** by,

Prof. Dr. Halil Kalıpçılar
Dean, Graduate School of **Natural and Applied Sciences** _____

Prof. Dr. Erdem Canbay
Head of the Department, **METU** _____

Assist. Prof. Dr. Cüneyt Baykal
Supervisor, **Civil Engineering, METU** _____

Dr. Hasan Gökhan Güler
Co-Supervisor, **Civil Engineering, METU** _____

Examining Committee Members:

Prof. Dr. Ahmet Cevdet Yalçıner
Civil Engineering, METU _____

Assist. Prof. Dr. Cüneyt Baykal
Civil Engineering, METU _____

Assoc. Prof. Dr. Mustafa Tuğrul Yılmaz
Civil Engineering, METU _____

Assist. Prof. Dr. Gülizar Özyurt Tarakcıoğlu
Civil Engineering, METU _____

Assist. Prof. Dr. Doğan Kısacık
Civil Engineering, IZTECH _____

Date: 24.08.2022

I hereby declare that all information in this document has been obtained and presented in accordance with academic rules and ethical conduct. I also declare that, as required by these rules and conduct, I have fully cited and referenced all material and results that are not original to this work.

Name Last name: Berkay Akyol

Signature :

ABSTRACT

A PHYSICAL MODEL STUDY ON REINFORCEMENT OF A BREAKWATER CONSISTING OF TETRAPOD ARTIFICIAL BLOCKS

Akyol, Berkay
Master of Science, Civil Engineering
Supervisor: Assist. Prof. Dr. Cüneyt Baykal
Co-Supervisor: Dr. Hasan Gökhan Güler

August 2022, 97 pages

The breakwaters of a commercial port in the Western Black Sea were extensively damaged as a result of a major storm that hit on January 18–19, 2018. As an urgent precaution, the breakwaters were repaired based on pre-damaged sections, but there is still a need to reinforce these breakwaters to avoid damage in the case of potential future storms. Wind and wave climate studies were conducted using long-term wind data from various sources, and deep-sea wave characteristics were transformed to the nearshore in order to be used in the design of reinforcing sections of breakwaters. It was decided to place 48-ton antifer blocks on the armor layer with a packing density of 0.61, which was constructed by using 24-ton tetrapod blocks before the damage caused by a storm, in order to reinforce the breakwater sections. The reinforced sections were scaled and tested in the wave channel of the METU Civil Engineering Department Coastal and Ocean Engineering Laboratory under wave conditions with different water levels and various recurrence periods determined by taking the local wave climate into account. Measurements regarding the stability of the structure and wave overtopping were performed. It was observed that the cross-section reinforced with antifer blocks work efficiently based on the toe design, and the section was finalized by trying different toe design alternatives. It has been

observed that the reinforced section is stable under design and overload wave conditions and wave overtopping is at acceptable levels.

Keywords: breakwater, tetrapod, antifer, reinforcement, wave overtopping

ÖZ

TETRAPOD YAPAY BLOKLARDAN OLUŞAN DALGAKIRANLARIN GÜÇLENDİRİLMESİ ÜZERİNE FİZİKSEL MODEL ÇALIŞMASI

Akyol, Berkay
Yüksek Lisans, İnşaat Mühendisliği
Tez Yöneticisi: Dr. Öğr. Üyesi Cüneyt Baykal
Ortak Tez Yöneticisi: Dr. Hasan Gökhan Güler

Ağustos 2022, 97 sayfa

Batı Karadeniz'de bulunan ticari bir limanın dalgakıranları, 18-19 Ocak 2018 tarihlerinde Karadeniz'de gerçekleşen güçlü bir fırtına sonucunda ağır hasar almıştır. Acil bir önlem olarak, dalgakıranlar hasar öncesi kesit tasarımları kullanılarak tamir edilmiştir, ancak bu dalgakıranların gelecekteki muhtemel fırtınalar sırasında hasar almaması için güçlendirilme ihtiyacı duyulmuştur. Dalgakıranların güçlendirme kesitlerinin tasarımında kullanılmak üzere; farklı kaynaklardan alınan uzun dönemli rüzgâr verileri kullanılarak rüzgâr ve dalga iklimi çalışmaları gerçekleştirilmiş, derin deniz dalga özellikleri yakın kıyıya taşınarak tasarıma esas dalga özellikleri belirlenmiştir. Dalgakıran kesitinin güçlendirilmesi için hasar öncesinde 24 tonluk tetrapod bloklar kullanılarak inşa edilen koruma tabakasının üzerine 48 tonluk antifer blokların yerleştirme sıklığı 0.61 olacak şekilde yerleştirilmesine karar verilmiştir. Güçlendirilen kesit ölçeklenerek ODTÜ İnşaat Mühendisliği Bölümü Kıyı ve Liman Mühendisliği Laboratuvarında bulunan dalga kanalında, yörenin dalga iklimi dikkate alınarak belirlenen farklı su seviyeleri ve farklı yineleme dönemlerine sahip dalga koşulları altında test edilmiştir. Gerçekleştirilen deneylerde yapının stabilitesi ve dalga aşaması ile ilgili ölçümler gerçekleştirilmiştir. Deneylerde, antifer bloklar ile gerçekleştirilen güçlendirmenin verimli olarak

çalışabilmesi için topuk tasarımının en iyi şekilde yapılması gerektiği görülmüş ve farklı alternatifler denenerek kesit son haline getirilmiştir. Güçlendirilen kesitin tasarım ve aşırı yükleme dalga koşulları altında hasar almadığı ve kabul edilebilir seviyelerde dalga aşmasının gerçekleştiği görülmüştür.

Anahtar Kelimeler: dalgakıran, tetrapod, antifer, güçlendirme, dalga aşması

To my family and beloved ones

ACKNOWLEDGMENTS

I would like to express my appreciation to my supervisor Assist. Prof. Dr. Cüneyt Baykal and co-supervisor Dr. Hasan Gökhan Güler for their guidance, advice, criticism, encouragement, and insight throughout the research.

I would like to express my sincere thanks to Prof. Dr. Ayşen Ergin for the education I received, for motivating me to learn amazing knowledge, and for letting me be part of this Coastal and Ocean Engineering family. I would like to convey my gratitude to Prof. Dr. Ahmet Cevdet Yalçıner, Dr. Işıkhan Güler, and Dr. Gülizar Özyurt Tarakcıoğlu for the education I received from them.

I would like to thank the technical assistant Yusuf Korkut to help me whenever I need and Eyüp Uğur for his effort to build my experimental setup. I also would like to thank Nuray Emre and Tanzer İlaslan for their support during my thesis study.

I would like to thank my friends Koray Göral, Emre Yıldırım, Mert Yaman and Kadir Karakaş for their help in learning how to use the tools in the flume. I would like to thank all my friends in coastal engineering family Akdeniz İnce, Aslıhan Devran, Barış Ufuk Şentürk, Berkay Erler, Bilge Karakütük, Can Özsoy, Cem Bingöl, Cem Sevindik, Ghazal Khodkar, Gökçe Ömeroğlu, Gözde Güney Doğan Bingöl, Günay Gazaloğlu, Furkan Demir, İlker Çoban, Kadir Karakaş, Mustafa Gökay Altunbaş, Sedat Gözlet, Utku Uzun, and Yağız Arda Çiçek for their presence in my life and all the memories that we shared.

I would like to give my sincere thanks to Burak Güngör, Mustafa Berkay Akpınar, and Taylan Utkurak, for helping me and giving me motivation.

I would like to give my deepest gratitude to my family for their support.

This study was funded by ODTU DOSIM Projects No: 19-03-03-2-02-223 and 21-03-03-2-02-035.

TABLE OF CONTENTS

LIST OF TABLES

TABLES

LIST OF FIGURES

FIGURES

LIST OF ABBREVIATIONS

ABBREVIATIONS

DHI	Danish Hydraulic Institute
JONSWAP	Joint North Sea Wave Project
CS-A	Cross-section alternative of Section 4-4
CS-B	Cross-section alternative of Section 2-2
SWL	Still water level
MWL	Mean water level
LWL	Low water level
HWL	High water level

LIST OF SYMBOLS

SYMBOLS

Ae	Eroded area
B	Width of area
d	Water depth
D_n	Nominal diameter of the unit
D_{n50}	Median stone size diameter
$D_{n50,toe}$	Nominal grain diameter of stones used in toe
$D_{n50,antifer}$	Nominal diameter of antifer blocks
Fr	Froude number
Fr_p	Prototype Froude number
Fr_m	Model Froude number
g	Gravitational acceleration
H_{max}	Maximum wave height
H_{m0}	Spectral significant wave height
H_s	Incident significant wave height
K_D	Stability coefficient.
L	Length of the area on the slope
L_m	Length in model
L_p	Length in prototype
m	Bed slope

N	Number of waves
Nb	Number of blocks in a defined area
N_{od}	Relative damage level in armor layer
$N_{od,toe}$	Relative damage level in toe layer
$N_{s,armor}$	Total number of displaced antifer units in the armor layer
$N_{s,toe}$	Total number of displaced antifer units in the toe
q	Wave overtopping discharge
S	Rear side damage parameter
S_{ave}	Maximum measurement of rear side damage parameter
S_{max}	Average measurement of rear side damage parameter
T_s	Significant wave period
T_m	Mean wave period
$T_{m-1,0}$	Spectral mean wave period
T_p	Spectral peak wave period
u	Velocity
Δx	Distance between two-point measurements
λ_L	Model length scale
λ_T	Model time scale
λ_W	Model weight scale
λ_ρ	Material density
λ_D	Armor diameter factor

λ_{Δ}	Relative mass density
ϕ	Packing density

CHAPTER 1

INTRODUCTION

Coastal areas are used for many purposes both by governments and private corporations. One of the important uses is related to the cooling of and transporting fuel to power plants. Therefore, many coastal protection structures are used to prevent severe harm to people and the structures behind them. the stability of these structures must be considered carefully A commercial port, located in the southwestern Black Sea along the Turkish coastline, suffered from excessive damage due to a severe storm on January 18-19, 2018. The plan view of the port is shown in Figure 1.1, indicating the locations of the breakwaters, and section numbers.

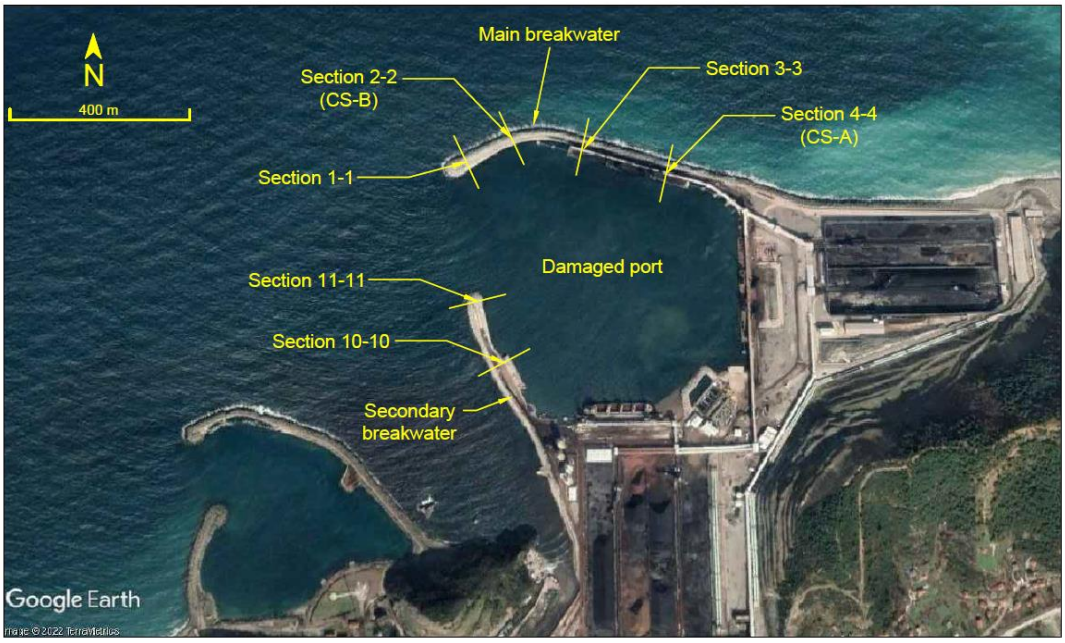

Figure 1.1: Layout of the damaged port

After this storm event, the main and secondary rubble mound breakwaters (the armor layer consisted of tetrapod units) of the port completely failed in Section 2-2 and Section 10-10 (see

Figure 1.1: Layout of the damaged port). Sections 1-1, 3-3, 4-4, and 11-11 of the breakwaters were also significantly damaged. The interested reader is referred to Guler et al. (2022) for a detailed discussion on the characteristics of the storm that caused the damage in this port in addition to the damage and failure mechanisms of the breakwaters. Urgent precautions had to be taken; therefore, the damaged breakwaters were repaired based on the designs of the rubble mound structures prior to the event as soon as possible. Meanwhile, the design wave parameters of the coastal defense structures were re-evaluated based on the recent databases and a possible reinforcement of these structures was considered.

In the reinforcement of the repaired breakwaters, adding a new armor layer on the existing cross-section without any extra rock filter layer in between the existing armor and the new armor is considered. Also, there was a need to decrease the wave overtopping to protect the conveyor belt and the other equipment at the harbor side. To decrease the wave overtopping, the crest levels were elevated with the artificial units. This study investigates the stability of the new armor layer, stability of the new toe design and its optimization, wave overtopping and its effects on rear side armor layer stability, and the effects caused by the placement of the armor layer on the crest.

In the study, first, the existing breakwater cross-sections were built. After that new reinforced design was constructed on top of the existing structure. The experiments were carried out for Section 4-4 and 2-2, separately. For both of the sections, the stability of the armor layer and toe design has been investigated, and also, the toe design was attempted to be optimized. For Section 4-4, the wave overtopping has been investigated. On the other hand, rear-side armor layer stability has been investigated for Section 2-2.

This study was performed to investigate the below given research questions.

(i) How is the performance of the antifer blocks placed directly on the tetrapods?

(ii) How does the toe design affect the overall structure stability and wave overtopping?

This study is structured as follows:

In Chapter 2, the literature on the damaged and reinforced breakwaters, and the antifer blocks will be given briefly.

In Chapter 3, the description of the existing breakwater and the design of new cross-sections will be explained briefly.

In Chapter 4, the description of the physical model experiments is presented. This chapter describes the wave channel and wave generator system, experimental setup and scaling, wave sets and water level conditions, construction of the cross-section, measurements, and experimental program.

The results of the experiments are given in Chapter 5. There are two main headings. The first one is related to the shallower cross-section (Section 4-4). In this part, damage to armor and toe layer in each alternative and overtopping discharges will be given. In the second part of this chapter, the results of the experiments of the deeper cross-section (Section 2-2) will be given. Damage on armor and toe layer in each alternative and measurement of rear side damage will be given.

In Chapter 6, a couple of discussion has been made about the results. These are the armor stability, toe stability, overtopping comparison, and rear side stability will be discussed.

In Chapter 7, a summary of what has been done so far and future remarks will be mentioned.

CHAPTER 2

LITERATURE REVIEW

There are many examples in the literature regarding the damages of the breakwaters caused by the storm and tsunami and the repair of these damages. When these examples are examined in terms of damage caused by storms in rubble-mound breakwaters, it will be seen that one of the most important examples is the Sines Harbor breakwater in Portugal (Baird et al., 1980). There exist two important examples from Turkey; The Antalya Port (Gunbak & Ergin,1985) and Giresun Port (Kilicoglu et al., 2004) breakwaters, which were heavily damaged after strong storms. The studies carried out in the examples -given are important as they reveal the mechanisms that cause damage to these breakwaters and the engineering measures that should be taken to prevent such damage in the future. However, there are a limited number of studies in the literature that include physical modeling studies for the elimination of such damages and the reinforcement of the breakwaters.

In this section, several damage cases in the literature are presented. After that the antifer unit that was used to reinforce the damaged breakwater is described.

2.1 Several cases of breakwater damages

An example of a well-prepared review study was done by Wiegel (1982). It gives extensive information regarding breakwater damage caused by severe storms and tsunami waves prior to 1982. However, this study mostly focused on rubble mound breakwater damages, which have been built using more slender artificial units like dolosse and tetrapod units, caused by severe storms, since the cross-section of concern in this study was built using tetrapod blocks.

One of the early recorded damaged breakwaters is Kahului Harbor Breakwater. Kahului Harbor is located on the north coast of the island of Maui. This harbor was protected by two rubble mound breakwaters (U. S. Army Corps, 1982). In 1956, this breakwater was reinforced by using 33-ton unreinforced tetrapod units below the 3.05 meters of mean lower low water up to the concrete cap after a severe storm in March 1954. However, again this breakwater has been damaged. To reinforce, two layers of 35-ton tribars had been placed lower third of the side slope whereas two layers of 50-ton tribars were placed upper two-thirds of the slope on top of the existing slope in 1966 (Sargent et al., 1988).

Another example of a damaged breakwater is Crescent City Breakwater. The damage occurred on the breakwater in February 1960. The damage was extensive breakage of 25-ton tetrapod units. To repair this breakwater, 40-ton dolosse were placed in 1973 (Magoon et al., 1974).

A well-known example in this scope is the Sines breakwater located in Portugal, which was constructed using 42 tons of non-reinforced dolosse units at the armor top on secondary armor layer consisting of 3-6 ton stones (ASCE Port Sines Investigation Panel, 1982) and damaged due to a storm in 1978. Although the design wave height was Hs = 11.0 meters and it was designed for 30-45 meters water depths, the damaging significant wave height was found between 8-9 meters (Ligteringen, 1987). One of the major reasons for the excessive damage was the overestimation of the mechanical strength of the dolosse units. The breakwater was repaired using 90 tons of antifer blocks placed on top of a recreated base of 6-12 tons of stones with a milder slope (Burcharth, 1987).

Another important example is the Arzew El Djedid breakwater located in Algeria, which was constructed using tetrapod units at the armor, and damaged due to a storm in 1980. The failure of the breakwater was related to the breakage of 48 tons of tetrapod units rather than hydraulic stability (Burcharth, 1987). The armor layer of this damaged breakwater was reinforced using 40 tons of antifer units. Furthermore, 60-65 tons of tetrapod units were placed on top of these antifer units (Gunbak,1999).

Another example is Tripoli Breakwater located in Libya, which was constructed using tetrapod units at the armor layer, and damaged due to a storm in 1981. The main reason for failure is that the design wave parameters were not found correctly (Maddrell, 2006). The breakwater was reinforced by installing a new parapet and adding a new layer of tetrapod units (the same size as the existing units) on the armor layer.

Another example is Antalya Harbor, located in Turkey. In the seaward armor layer, 9-15 tons of stones as two layers, and in the rear side armor layer, 2-6 tons of stones are used. This breakwater was damaged due to a storm event that occurred in 1971. The main reason for the damage is that the storm hit the breakwater while under construction process (Gunbak & Ergin, 1985). The breakwater was reinforced by placing two different rectangular concrete blocks, which have dimensions of 2x2x4m, and 2x2x5m, at the armor layer. The specific weight of concrete was taken as 2.4. Thus, smaller rectangular blocks weigh 38.4 tons, and larger rectangular concrete blocks weigh 48 tons. At the toe layer, heavier than 15 tons of stones were used.

Another example is Giresun Port, located in Turkey. In the armor layer 10-15 tons of stones are used. This breakwater was damaged significantly by a storm in 1999. The main reason for the damage is that the design wave parameters were not found correctly and appropriate maintenance was not carried out (Arıkan, 2010).

The final example to be given is the Richards Bay Breakwater. This breakwater has been made by using ton dolos units. This breakwater was damaged by a severe storm with an 8.5-meter wave height in March 2007. This wave height is greater than the design wave height (Domingo, 2012). Up until now, most of these damaged breakwaters consisted of dolosse and tetrapod units. One of the reasons for this is that there are not many different artificial units to build these breakwaters. Furthermore, both dolosse and tetrapod units will break earlier apart from their material strength due to slenderness. This problem was studied to obtain an empirical formula for the breakage of dolosse and tetrapod units (Burcharth et al., 2000).

Moreover, many breakwaters have been reinforced by using antifer units as well as studied commercial port breakwaters. Therefore, next subsection, the information related to antifer units will be given.

2.2 Antifer (Artificial Concrete Unit)

There are various artificial concrete units. However, to be able to use these units, some limitations and restrictions were available. Some of them have water depth restrictions whereas others have weight and length restrictions due to their slenderness. Therefore, these units were classified by shape, placement method, stability factor, and structural strength (Domingo, 2012). If one wants to use an artificial unit on existing artificial units, the limitation and classification should be carefully considered.

Usage of antifer blocks could be first seen in history between 1976 and 1978 for the Antifer Harbor of France. These antifer cube blocks, however, just stand up against the waves by their mass. No interlocking would be looked for like the tetrapods, dolosse, etc. They will be placed as two layer, so some damage would be allowed until the repair of the damage (Yagci & Kapdasli, 2003). Furthermore, like Xbloc, some units have a patent certificate. Thus, one cannot use it of their free will. To summarize why antifer cube blocks were selected, they can be used without paying another expense for the patent certificate and the mechanism works under their mass. Thus, even if some damage occurs, they can be repaired without failure of the section or breakwater which decreases the cost of maintenance. Since they do not have any size limitations, they can be used as heavier units without changing the stability of the unit. They can also be used at any depth.

The general features of an antifer block are given in Table 2.1.

Table 2.1: Geometric characteristics of antifer blocks (adapted Domingo, 2012).

Geometric Character	Expression	Symbol
Volume	The volume of the antifer	V
Bottom Width	$1.076 * \sqrt[3]{V}$	a
Top Width	$0.9254 * a$	b
Height	$0.921 * a$	h
Groove Radius	$0.115 * a$	r
Groove Depth	$0.0877 * a$	c
Corner Side Width	$0.022 * a$	s
Taper Angle	87.7°	B

A sketch is shown for oblique, plan views, and cross-section of an antifer block in Figure 2.1 (Yagci & Kapdasli, 2003).

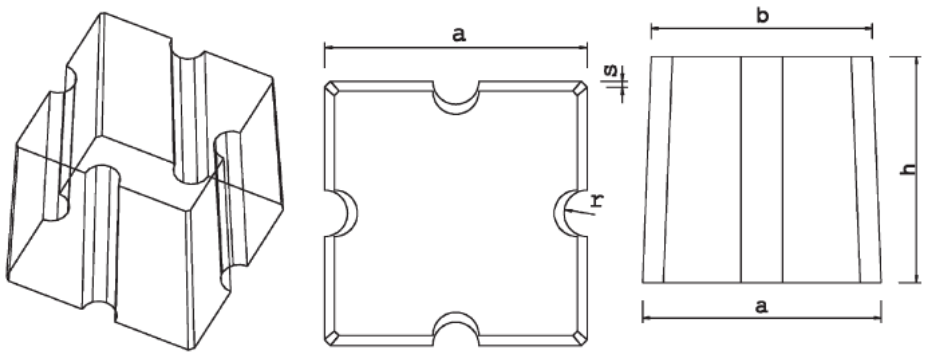

Figure 2.1: Oblique, plan, and cross-sectional drawings of an antifer block (adopted from Yagci & Kapdasli, 2003)

An example of used antifer blocks in the experiments is shown in Figure 2.2.

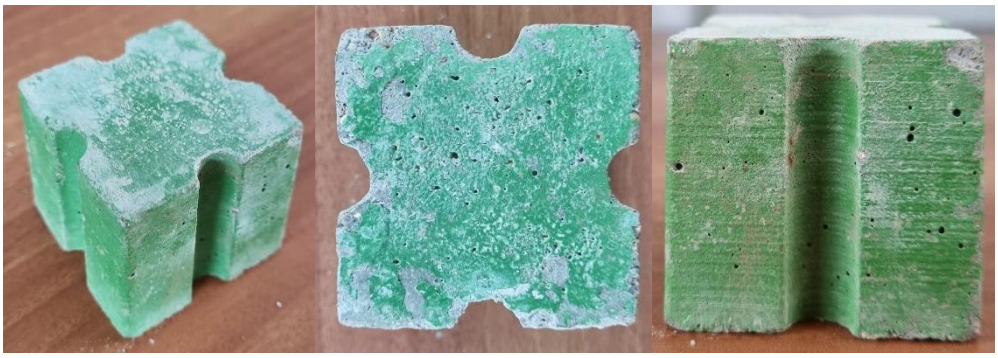

Figure 2.2: Oblique, plan, and cross-sectional views of antifer blocks used in the experiments

To determine the weight of an artificial unit, firstly, the stability coefficient (K_D), which takes account of many variables for all units, should be known. The most famous formula for calculating the weight of an armor unit is Hudson et al. (1979) given in Equation (2.1).

$$W = \frac{\gamma_s * H^3 * \tan\ \alpha}{(S_r - 1)^3 * K_D} \tag{2.1}$$

Where; W is the mean weight of armor unit (tons), γ_s is the saturated surface dry unit weight of armor unit, H is the design wave height at the construction depth, α is the angle of structure slope, and K_D is stability coefficient.

In the literature, the Coastal Engineering Manual (US Army Corps Of Engineers, 2002) defined placing density as the number of armor units per area. Moreover, packing density was described as the number of placed units per square nominal diameter by Van der Meer (1999). Reedijk and Muttray (2009) defined it in a similar way. Packing density (ϕ) could be defined as the percentage of actual blocks to the highest number of blocks per surface unit averaged per layer (Frens, 2007). It could be expressed as Equation (2.2).

$$\phi = \frac{Nb * D_n^2}{B * L} \tag{2.2}$$

Where Nb is the number of blocks in a defined area, B is the width of the area, L is the length (on the slope) of the area D_n is the nominal diameter of the unit.

In Figure 2.3, part of an example calculation of packing density is shown.

Figure 2.3: Packing density calculation process in the experiment

To obtain a more accurate stability coefficient, one should examine different placement methods. For antifer blocks, changing placement would result in different packing density ratios. Thus, a different stability coefficient would be acquired. In Table 2.2, a summary of the results of performed experiments is given (Frens, 2007).

In this Table2.2, one can see that by changing the placement method, obtained stability coefficient value differs for antifer blocks depending on packing density.

Table 2.2: Results of the performed experiments (adapted from Frens, 2007)

Packing densities around	***Placement Method***	***Experiment No.***	ϕ **(%)**	K_D
45%	Closed pyramid	14	44.8	4.1
50%	Column	6	49.1	16.3
	Column (under an angle)	8	50.0	9.4
	Closed pyramid	1	49.7	6.4
	Double pyramid ($0-?\ .D_n$)	12	49.1	4.0
	Filled pyramid	4	49.1	-
55%	Double pyramid ($1/2\ .D_n$)	11	54.3	16.4
	Closed pyramid	13	54.3	16.0
	Double pyramid ($3/4\ .D_n$)	15	53.9	15.9
	Double pyramid ($?-\ {}^{1}/_{4}\ D_n$)	10	53.2	15.7
	Double pyramid ($0-?\ .D_n$)	17	53.5	13.2
	Irregular (placed per layer)	16	57.4	9.7
	Irregular (placed per row)	2	57.0	9.4
	Column (irregular pos.)	3	54.2	4.0
60%	Double pyramid ($0-?\ .D_n$)	9	58.5	23.7
	Double pyramid (irregular pos.)	7	58.5	16.7
	Irregular (placed per layer)	5	61.1	16.3

So far in this chapter, detailed information about damaged breakwaters and how they were repaired were examined thoroughly. Moreover, it is found that the artificial unit to be used to repair the studied section is antifer blocks, which are easy to implement and commonly used in history to strengthen the breakwaters. The general features of its geometry, some advantages of its usage, the effects of different placement method, and its effect on stability was mentioned.

CHAPTER 3

DESIGN OF REINFORCED CROSS-SECTIONS

In this study, the reinforcement of the commercial port, located in the southwestern Black Sea along the Turkish coastline, was investigated. This breakwater was damaged by a severe storm on January 18-19, 2018. The breakwater had been repaired to the condition before the severe storm event. However, the breakwater should be reinforced so as not to be damaged by potential future storms.

In this research, two cross-sections were examined: Section 4-4 and Section 2-2. Section 4-4 had a water depth of approximately 20 meters at the toe of the structure, 0-400 kg core material, 0.4-2-ton stones first filter layer, and 2–4-ton stones second filter layer. The main armor layer was formed of 24-ton tetrapod units. The armor layer placed on a toe, which has 2–4-ton stones, has 16 meters of water depth in front. The rear side armor layer, which had 1-3-ton stones, was placed on top of the rear side filter layer having 0.4-1-ton stones. Whereas Section 2-2, had a water depth of approximately 30 meters at the toe of the structure, and 400 kg core material, the first filter layer had 0.4-2-ton stones. Above this layer, there was again another filter layer consisting of 2–4-ton stones. The main armor layer was formed with 24-ton tetrapod units. The armor layer placed on a toe, which has 4-6-ton stones, has approximately 19 meters of water depth in front. The rear side armor layer, which had 4-6-ton stones, was placed on top of the rear side filter layer having 2-4-ton stones. Other details of the existing breakwater could be seen in Figure 3.1.

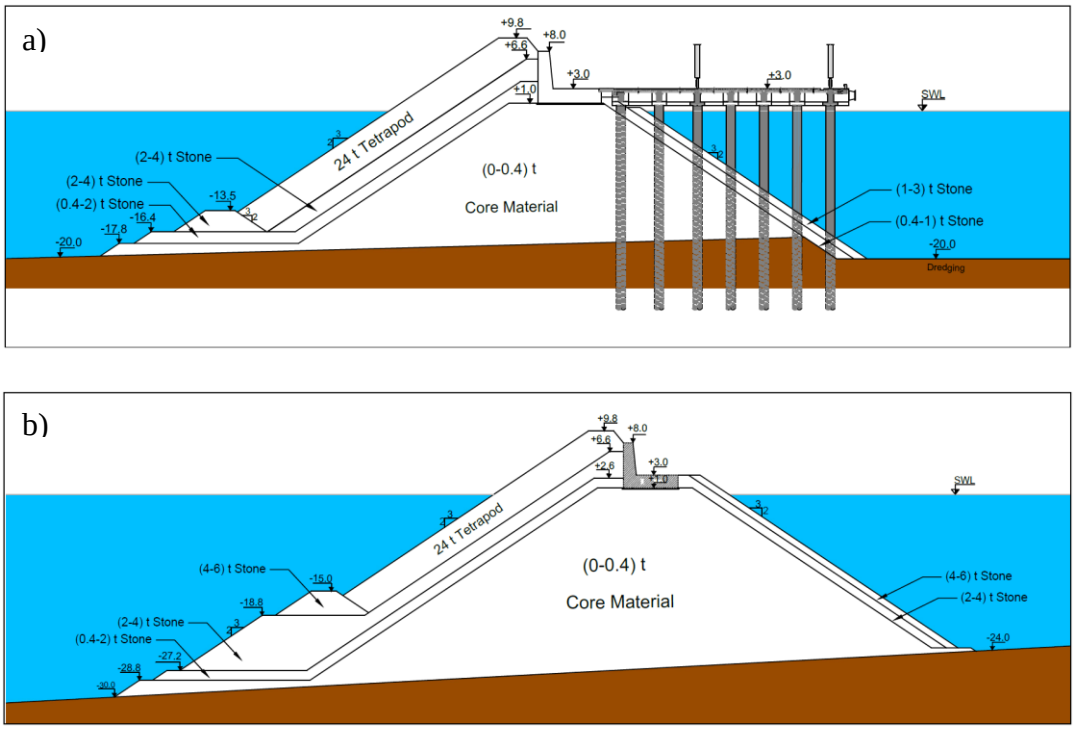

Figure 3.1: The original cross-sections along the main breakwater in prototype scale: a) Section 4-4 and b) Section 2-2

Before the design of reinforcement, firstly reasons for damages and wave conditions were examined, and design water levels and wave parameters were re-evaluated (METU, 2020). In this document, deep-water significant wave height (H_{s0}) and peak wave period (T_p) with a return period of R_p=100 years were given as H_{s0}=9.0 m and T_p=12.4 s, respectively. To calculate the nearshore wave characteristics at the toe of the breakwater, Simulating Waves Nearshore (The SWAN Team, 2019) numerical model was used considering the water level changes, which will be mentioned in more detail in Section 4.3. Upon investigating these water levels and wave characteristics, the most critical design condition was found in the case of a return period of R_p=100 years as the design significant wave height (H_{s0}) =8.6 m and the peak wave period (T_p) =12.4 s, respectively at the high-water level and at two wave lengths away from the main breakwater. The most critical design condition occurs in the North North West direction of the breakwater. By considering cost, ease of implementation, and reducing the risk of a decrease in stability factor due to the probability of not having enough interlocking between newly placed units, antifer

blocks were chosen to reinforce the breakwater. Other reasons for this selection are summarized in Chapter 2 of this thesis.

3.1 Description of tested cross-sections

To be able to determine the weight of artificial armor unit, one should know its stability coefficient. In the literature review part of this thesis, it was mentioned that by changing the placement method with a related packing density ratio, one can obtain a different stability coefficient (Frens, 2007). By using this approach, the stability coefficient of antifer units was determined for a packing density of 0.61. Since the stability coefficient value is directly related to the packing density of armor units, one should carefully check the packing density of experiments. As mentioned in Guler et al. (2022), wave overtopping will increase drastically for the original design also with newly estimated design wave characteristics.

Since removing the existing 24 tons of tetrapod unit is a difficult task and not a cheaper solution than reinforcing with another unit, it is determined that the breakwater will be reinforced with antifer units, the more details about this selection were mentioned in the literature review part of this thesis.

For Section 4-4 (shallower section), to decrease overtopping 42-ton cubes were placed on 2–4-ton stones on the toe. To increase the stability of the armor layer, 48-ton antifer blocks were placed on existing 24-ton tetrapod units irregularly with a 0.61 packing density (Frens, 2007). In irregular placement, the antifers were placed in such a way that any side or corner of the antifers was touching tetrapods. The irregular placement on the slope and the regular placement at the crest are shown in Figure 3.2, Figure 3.3, and Figure 3.4.

Furthermore, to decrease cost while decreasing wave overtopping without enlarging the crown wall, antifer units were placed regularly on the crest to simulate a crown wall structure. In regular placement, the antifers were placed such that the bottom sides were touching the filter layer.

Figure 3.2: Closer look at the seaside view of an example cross-section used in the experiments

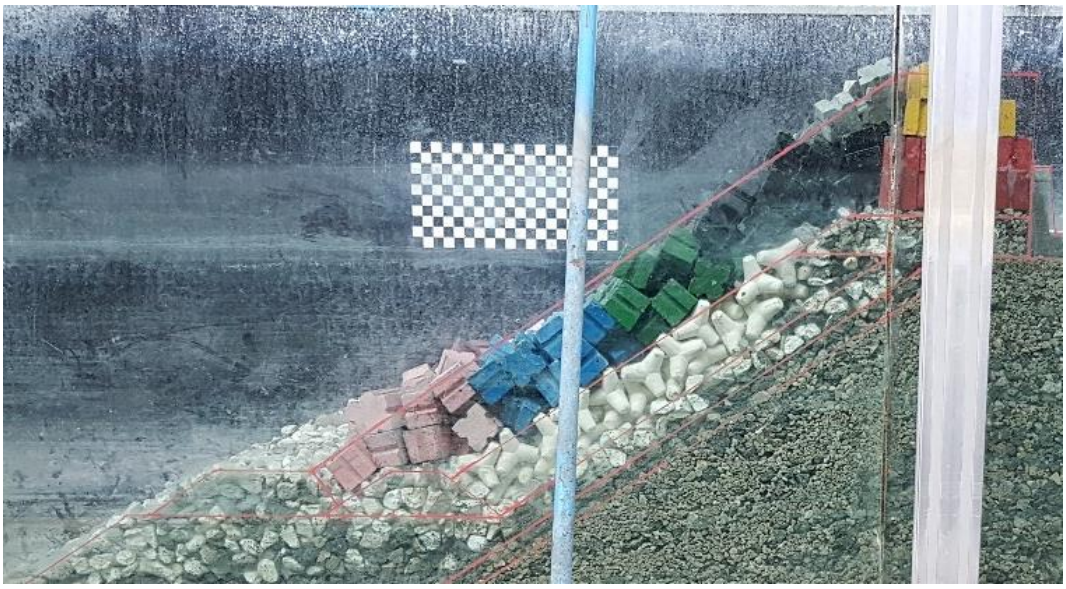

Figure 3.3: Side view of the sample cross-section

Figure 3.4: Rearside (left) and seaside (right) views of an example cross-section used in the experiments

The crest height of the regularly placed antifer units is set to +14.9 m for both Section 4-4 and Section 2-2. Thus, to implement these changes, the highest level of the tetrapod units was lowered to +1.0 m for both the sections and 2-4 t stones were positioned on top of the tetrapod units in two layers to serve as a base for the antifer units that were placed regularly. The regularly placed antifer acts like a crown wall for the irregularly placed antifer units in the armor layer. Furthermore, since there is a conveyor on the rear side in Section 4-4, existing 1–3-ton stones were used at rear side armor layer. In Figure 3.5, the first tested alternative was shown.

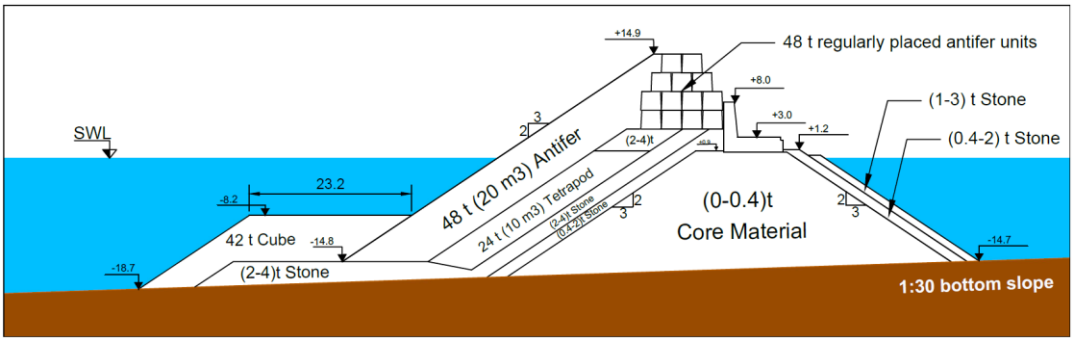

Figure 3.5: Cross-section of the first alternative for Section 4-4 given in prototype scale

The same principles were applied in Section 2-2. With a 0.61 packing density of antifer units, the armor layer leaned on regularly placed antifer blocks at the crest. Section 2-2 is relatively deeper than Section 4-4. Therefore, firstly, 4–6-ton stones were placed on the toe at a deeper depth. Since there were some damages on the rear side armor layer in Section 4-4 due to wave overtopping, the armor layer on the rear side was reinforced with 4–6-ton stones. In Figure 3.6, the first tested alternative of the deeper section was shown.

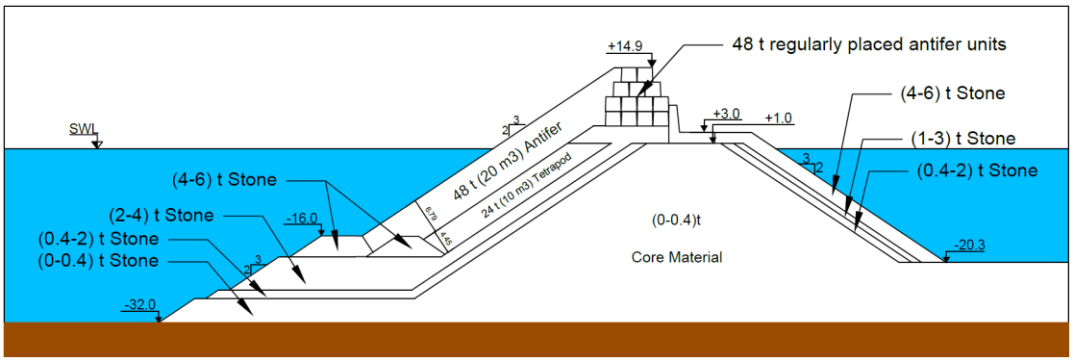

Figure 3.6: Cross-section of the first alternative for Section 2-2 given in prototype scale

In this study, from this point on, Section 4-4 will be referred to as Cross-section A and shown with CS-A, and Section 2-2 will be referred to as Cross-section B shown as CS-B. Thus, it is believed that the alternative (modified) cross-sections can be grouped in an easier way.

CHAPTER 4

DESCRIPTION OF THE PHYSICAL MODEL EXPERIMENTS

4.1 Wave channel and wave generator system

The net length of the channel is 20.6 m excluding the wave generator and wave absorbers. The experiments were carried out in two inner channels (18 m long with 0.6 and 0.9 m widths), built into a 6.0 m wide, 1.0 m deep irregular wave channel located in the Middle East Technical University, Civil Engineering Department, Coastal and Ocean Engineering Laboratory (see Figure 4.1). In this channel, between 0.4 and 0.7 m, water depth and irregular waves having 0.5 s and above wave period and up to 0.20 m significant wave height could be generated.

Figure 4.1: METU Civil Engineering Department, Coastal and Ocean Engineering Laboratory, Irregular Wave Channel.

In addition to irregular waves, user-defined water surface time series (storm recordings, solitary waves, etc.) and regular waves could be generated in the channel. The wave generation system is a 6 m wide single block piston-type wave generation system manufactured by the Danish Hydraulic Institute (DHI) (Figure 4.2).

Figure 4.2: Piston type wave generator

By the installation of plywood, the seabed profile of 1:30 at the region was represented. On the right side of the inner flume, the seabed was constructed as plywood, and to reflect the effects of surface roughness of the bed slope, oil paint was used to bond sand to the plywood (see Figure 4.3), similar to Eldrup et al. (2019) who glued small size stones on a plywood. .

Figure 4.3:Wave channel and inner wave flume

4.2 Experimental setup and scaling

As mentioned in Chapter 3, Section 4-4 will be referred to as Cross-section A and denoted as CS-A, and Section 2-2 will be referred to as Cross-section B and denoted as CS-B. In Figure 4.4, the positions of wave gauges and the experimental setup are shown for CS-A. The center of this channel is the intersection of the wave generator (positioned at x=0) and the still water level (SWL). The vertical axis is shown with the y-axis. In this study, the still water level is the local annual mean water level.

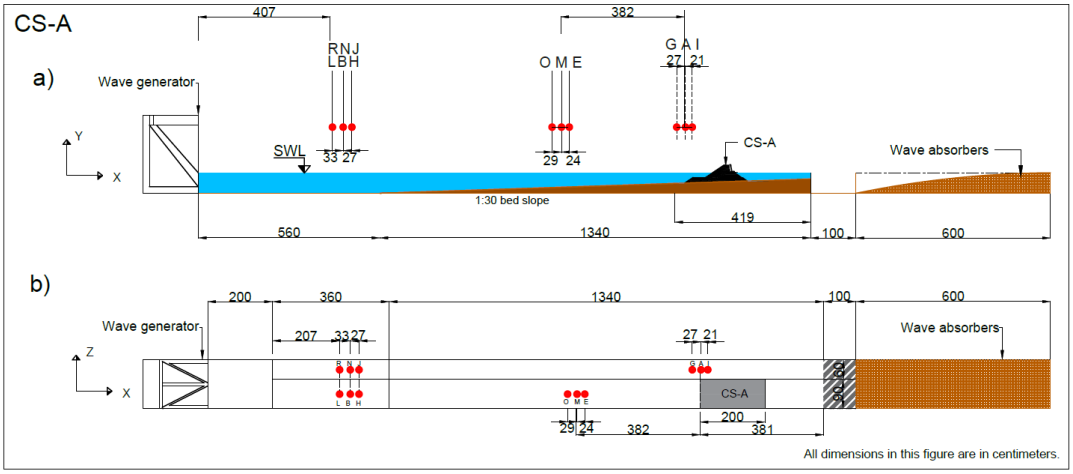

Figure 4.4: Positions of wave gauges and layout of experimental setup for CS-A experiments (Dimensions are given in centimeters. a) Side view, b) Top view.)

In Table 4.1, each wave gauge's names, locations, water depths, and distances from the toe were given for CS-A.

Table 4.1:For the CS-A wave gauges' locations, names, and water depths (at model scale) with respect to still water level (SWL).

Wave gauge		Channel without a section		Channel with a section	
		Distance from toe (cm)	Water depth-SWL (cm)	Distance from toe (cm)	Water depth-SWL (cm)
Toe	G	24	32.0	-	-
	A	3	31.1	-	-
	I	24	30.4	-	-
Off-Shore	L-R	1112	63.6	1112	63.6
	B-N	1079	63.6	1079	63.6
	H-J	1052	63.6	1052	63.6

In Figure 4.5, the positions of wave gauges and the experimental setup are shown for CS-B. For CS-B, wave calibrations are done by making experiments until measured wave data at the position of the GAI wave gauge group and targeted wave characteristics are nearly identical. When these wave characteristics were the same wave calibrations were accepted as completed.

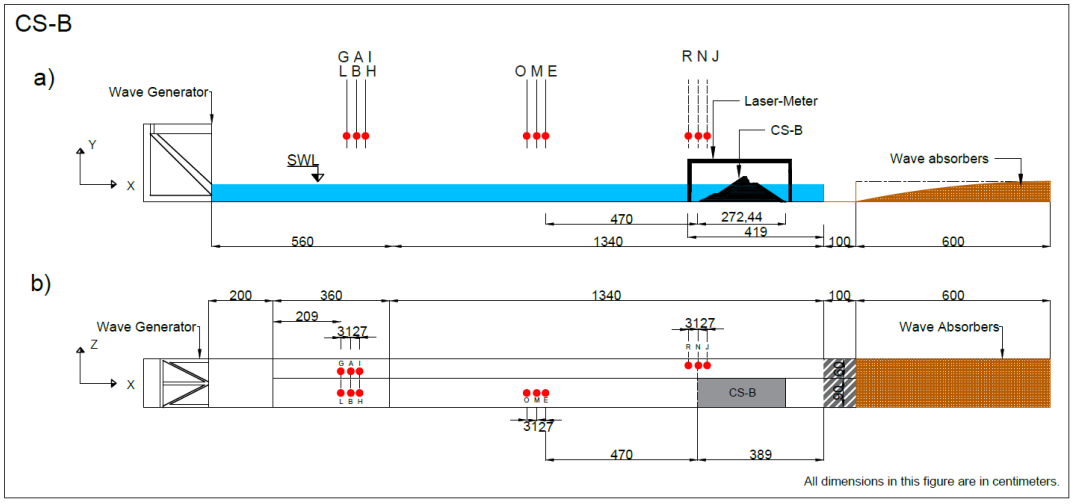

Figure 4.5: Positions of wave measurements and layout of sections for CS-B experiments (Dimensions are given in centimeters. a) Side view, b) Top view.)

In Table 4.2, names, locations, water depths, and distances from the toe of the wave gauges used in CS-B experiments were given.

Table 4.2: For CS-B wave gauges' locations, names, and water depths (at model scale) with respect to still water level (SWL).

Wave gauge		Channel without a section		Channel with a section	
		Distance from toe (cm)	Water depth-SWL (cm)	Distance from toe (cm)	Water depth-SWL (cm)
Toe	R	29	53.3	-	-
	N	1	53.3	-	-
	J	29	53.3	-	-
Off-Shore	L-G	1102	53.3	1102	53.3
	B-A	1071	53.3	1071	53.3
	H-I	1044	53.3	1044	53.3

In the case of CS-A, three wave gauges (G, A, I) are positioned at the toe of the structure and, another three gauges (R, N, J) are positioned the same offshore of the channel. Furthermore, another three gauges (L, B, H) are placed in the channel with the section in line with RNJ wave gauges. For CS-B, three wave gauges (R, N, J) are positioned at the toe of the structure and, another three gauges (G, A, I) are positioned at the offshore in line with LBH wave gauges.

Water surface elevations measured by wave gauges were acquired through the software developed by TDG Scientific Measuring Ltd. (2016). Reflection, spectral, and time domain analysis of time series transferred to computer environment were done with software developed by METU, Civil Engineering, Coastal, and Ocean Engineering Research Center. The wave absorbing system used in this channel is passive type. The Mansard and Funke (1980) method, which uses the data of three wave gauges placed at specific intervals, was used in the analysis of the waves reflected from the structure and the wave generator in the channel. After the wave analysis, incident spectral and zero-up crossing wave characteristics, which are significant wave height (H_s), maximum wave height (H_{max}), significant wave period (T_s), spectral significant wave height (H_{m0}), spectral mean wave period ($T_{m-1,0}$) and spectral peak wave period (T_p) were found. the number of waves in the all-wave series (N) was obtained using the zero-up crossing method.

Wave gauges were calibrated daily before and after the experiments. Moreover, the procedure to calibrate wave is done as follows. Wave calibrations are done by making experiments until the differences between obtained wave data at the position of the specific wave gauge group (LBH for CS-A and GAI for CS-B) and targeted wave characteristics are nearly identical. When these wave characteristics are the same, wave calibrations were accepted as completed.

The damage in the cross-sections were evaluated based on the dislocation and rocking of artificial stones on the breakwater section. The dislocation and rocking of these artificial units were determined by using photos and videos of the experiments.

The videos were recorded using a Sony RX0 camera. The experimental setup for the laser-meter and video recorder is given in Figure 4.6.

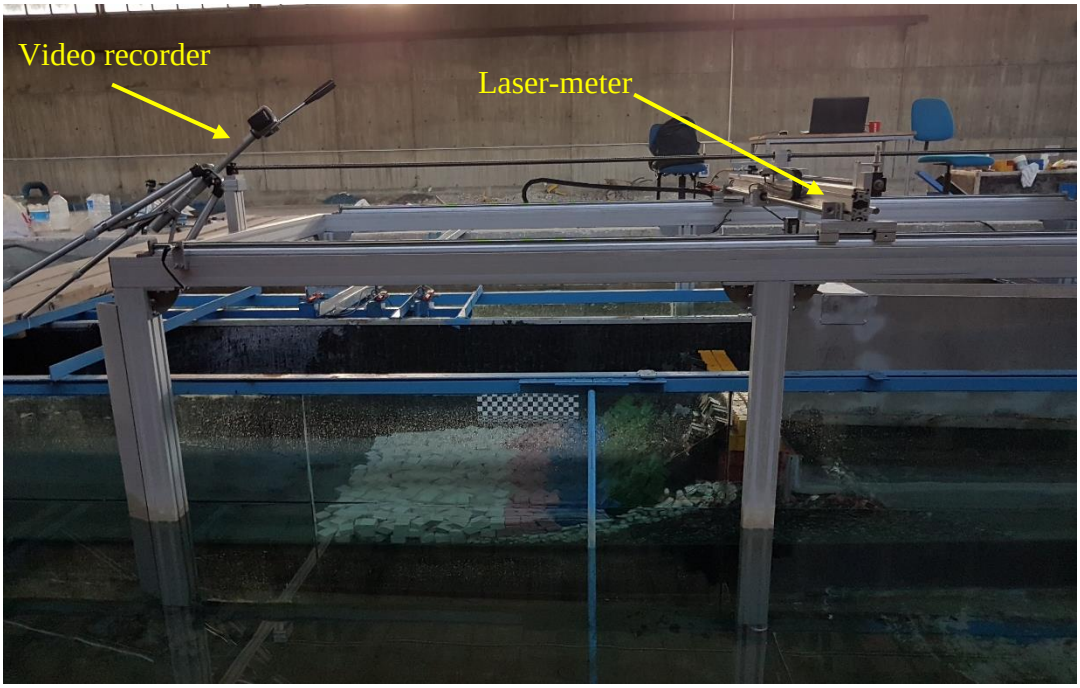

Figure 4.6: Video recorder and laser-meter setup

Since these experiments were done during day and night, a lighting system was implemented not to miss any recording and to visualize the experiments in a better way. This lighting system could be seen in Figure 4.7.

Figure 4.7: Lighting System

In physical model studies, where gravitational and inertial forces are effective, such as breakwater stability and wave overtopping discharge, where the movements and effects of sea waves, Froude theory is used to determine the model scale (Hughes, 1993). The Froude number is defined as the ratio of the water particle velocity (u) squared over the product of the characteristic length (water depth, d for current experiments) and the gravitational acceleration (g) ($Fr=u^2/gd$). According to the Froude theory, the Froude numbers in the prototype and the model must be equal ($Fr_m=Fr_p$; the lower letters "p" and "m" represent the words prototype and model). The geometric similarity in the model is achieved by equating the ratio of the value

(L_m) of each variable whose dimension is the length in the model and its actual values (L_p) to the model scale (λ_L). The time scale (λ_T) is given as the square root of the length scale according to Froude's theory ($\lambda_L = \lambda_T^{0.5}$).

According to Hydralab (2007), commonly used physical breakwater model scales are 1:5 to 1:80. For typical 2D experiments, between 1:30 and 1:60 scale is used. Although it is preferable to use a large scale, considering the limitation of irregular wave piston capacity and channel dimensions, a 1:60 length scale was selected. The weight scale (λ_W) was determined using the formula given in Eq. 4.1 (Hudson et al., 1979), which was also recommended by Hydralab (2007).

$$\lambda_W = \lambda_\rho * (\lambda_D)^3 = \lambda_\rho * (\frac{\lambda_L}{\lambda_\Delta})^3 \tag{4.1}$$

λ_W shows weight scale factor, λ_ρ is the material density, λ_D is armor diameter factor, λ_Δ is relative mass density and λ_L is the length scale.

In the experiments, to minimize scale effects caused by viscosity in determining the dimensions of the stones used in the core layer, the approach given by Burcharth et al. (1999) was used.

In Table 4.3, section, model scale, artificial units, rock properties, and scaling properties were given. Common parts of the two experiments were given first. After that specific differences were given for CS-A. Then other specific parameters were given for CS-B. The variables in the table could be expressed as the prototype density of concrete is 2400 kg/m^3, the density of seawater is 1018 kg/m^3, the density of the stones to be used in the filter and core layers in the prototype is 2700 kg/m^3, and the density of the water to be used in the laboratory is 1000 kg/m3. The density of the artificial units to be used in the experiments is 2360 kg/m^3, and the density of the stones to be used in the filter and core layers is approximately 2650 kg/m^3. By using these parameters, the weight scale providing the dynamic simulation conditions was determined. The 48-ton antifer, 24 tons tetrapod, and 48 and 10 tons cube artificial

blocks in the prototype were scaled to antifer weighing 218.5 grams, tetrapod weighing 109 grams, and cubes weighing 190.7 and 45.3 grams in the laboratory environment, respectively. It was determined that model units should be used. In order to produce tetrapod, antifer, and cube artificial blocks in specified dimensions, molds were prepared as discussed in this section.

Table 4.3:Physical model test scale, stone properties

Condition	Variables	Prototype	Model
Common	The density of water (kg/m^3)	1018	1000
	The density of concrete (kg/m^3)	2400	2360
	Antifer weight	48 (ton)	218.5 (gram)
	Tetrapod weight	24 (ton)	109 (gram)
	Stone weight	2-4 (ton)	9-18 (gram)
	Stone weight	1-3 (ton)	4-13 (gram)
	Stone weight	0.4-2 (ton)	2-11 (gram)
	Stone weight	0.4-1 (ton)	2-6 (gram)
	Stone weight*	0-0.4 (ton)	0-8 (gram)
CS-A (Section 4-4)	Cube weight	42 (ton)	190.7 (gram)
	Water depth in front of the toe with respect to still water level(m)	11.2	0.187
CS-B (Section 2-2)	Cube weight	10 (ton)	45.3 (gram)
	Water depth in front of the toe with respect to still water level(m)	32	0.533
	Stone weight	4-6 (ton)	18-27 (gram)
	Stone weight	6-8 (ton)	27-36 (gram)
	Stone weight	8-10 (ton)	36-45 (gram)
**In the experiments. when determining the dimensions of the 0-0.4-ton stones used in the core layer. the approach given by Burcharth (1999) was used to minimize the scale effects caused by viscosity.*			

As a result of the examinations made in the strengthening section designed for CS-A, it was decided that it would be appropriate to place 48 tons of antifer units on the existing tetrapod units. In the first alternative section studied, it was decided to use

cube units weighing 42 tons at the toe of the structure. For the CS-B, again, it was decided to place 48 tons of antifer units on the existing tetrapod units on the armor layer. On the toe, firstly, 4-6 tons of stones were used.

4.3 Wave set and water level conditions

In order to observe the cumulative damage conditions on the breakwater trunk section in physical model experiments, the wave conditions, which both the prototype and model properties were given in Table 4.4, were considered in the experiments. Wave conditions consist of six storms. In determining the characteristics of wave conditions, the results of the wave climate studies (METU, 2022) were considered. The reason why the order of this wave set was implemented (moderate storms to severe storms) is most likely the moderate storms will happen before the severe storms.

Table 4.4: Wave set

Wave Cond.	**Exceed. Prob. /Return Period**	**Prototype Scale**		**Model Scale**		**# of Waves (N)**	**Water Level (m)**
		Significant Wave Height H_{m0} (m)	**Significant Wave Period T_s(s)**	**Significant Wave Height H_{m0} (m)**	**Significant Wave Period T_s(s)**		
D1	10 hrs./yr.	5.4	9.65	0.090	1.25	2763	MWL (+0.12)
D2	5 yr.	6.9	10.32	0.115	1.33	3445	MWL (+0.19)
D3	50 yr.	8.1	11.21	0.135	1.45	3965	MWL+(0.23)
D4-1	100 yr.	8.6	11.52	0.143	1.49	3858	LWL (+0.13)
D4-2	100 yr.	8.6	11.52	0.143	1.49	3858	HWL (+0.95)
D5	100 yr. **	9.2	12	0.153	1.55	3704	HWL (+0.98)
** Design water levels are given with respect to SWL (local annual mean water level).*							
*** Upper limit of 90% confidence band,* *The name of wave conditions is shown as 'wave cond.', hours as a hrs. year as a yr.*							

In this study, the water level changes were studied in detail for the breakwater location and were calculated by considering tides, seasonal changes, water level changes due to climate change, and barometric and Coriolis effects (METU, 2020).

All wave conditions consist of a succession of randomly generated series of irregular waves. The JONSWAP spectrum $(peak\ enhancement\ factor,\ \gamma = 3.3)$ was used to generate the wave series. Empty channel tests were performed for wave calibration within the test channel before the sections were placed in the channel. The wave series determined after these experiments were used in the experiments to be made with the cross-sections.

In the experiments, the first wave condition (D1) has a probability of exceeding 10 hours a year. D1 is considered the wave condition that can be expected every year and corresponds to the service conditions. The properties of this wave condition are given in Table 4.4. D1 wave condition is given as the highest significant wave height in front of the breakwater structure from the West and West-North-West directions. D1 wave condition was applied as a random wave train of 2763 individual waves. This number of waves corresponds to approximately 6 hours in the prototype (when calculated by taking T_m=T_s/1.16; Goda, 2000). The water level in this wave condition is the water level 0.12 m above the still water level in the prototype.

Following the D1 wave condition, the D2 wave condition (significant wave height with a recurrence period of 5 years) was applied without repairing the damage to the structure). The water level in this wave condition is the water level 0.19 m above the still water level in the prototype. The D2 wave condition was applied as 3445 waves in the experiments. This time corresponds to about 8 hours in the prototype.

After the D2 wave condition, the D3 (H_{m0} = 8,1 m) wave condition, which has a significant wave height that can be observed in wave conditions with a 50-year recurrence period without repairing the damages to the structure, was applied). The water level in this wave condition is the water level is 0.23 m above the still water level in the prototype. The D3 wave condition was applied as 3965 waves in the experiments. This time corresponds to about 10 hours in the prototype.

Again, without repairing the damages to the breakwater, the D4-1 (H_{m0} = 8,6 m) wave condition, which is the highest wave height in front of the structure, at the low water level can occur under wave conditions with a recurrence period of 100 years, was applied around the breakwater structure. This wave condition was applied at a low water level. This water level is 0.13 m above the still water level in the prototype. The D4-1 wave condition corresponds to the design significant wave height at the low water level. It was decided to send the D4-1 wave condition as 3858 number of waves. This time corresponds to about 10 hours in the prototype.

After the D4-1 wave condition, The D4-2 wave condition, which is defined as significant wave height with a 100-year recurrence period in high water level, was applied. The number of waves was accepted as 3858. The duration of the storm is approximately 10 hours in the prototype. The water level for the D4-2 wave condition is the water level 0.95 m above the still water level in the prototype.

The last wave condition in the wave set is D5. The D5 wave condition could be expressed as significant wave height with a 100-year recurrence period corresponding to the overload condition in the high-water level. The number of waves was accepted as 3704. The duration of the storm is approximately 10 hours in the prototype. The water level for the D5 wave condition is the water level 0.98 m above the still water level in the prototype. All wave conditions were applied consecutively from D1 to D5 without reparation of damage.

4.4 Constructing the cross-sections

In this chapter, the two important topics, which are artificial unit manufacturing and packing density, will be given related to the construction process since these topics have not been explained in detail in the literature.

4.4.1 Artificial units manufacturing

To manufacture tetrapod, antifer, and cube units with the desired dimension more accurately, a 3-D printer, the Anycubic i3 mega model, was used to prepare the mold. In Figure 4.8, the Anycubic i3 mega 3-D printer could be seen.

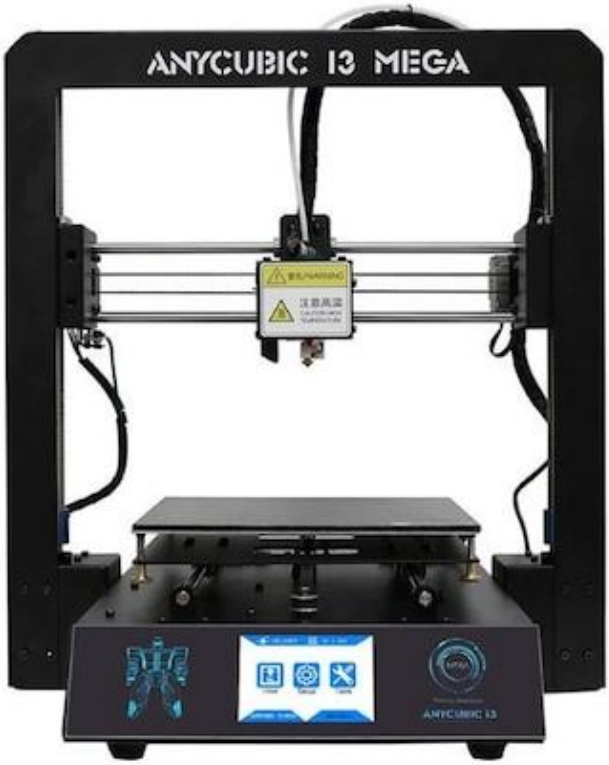

Figure 4.8: Anycubic i3 mega model 3-D printer

To be able to manufacture artificial units, there are a couple of steps. The first one is scaling mentioned in Section 4.2 Another one is to have molds, which are used in the experiments, given in Figure 4.9.

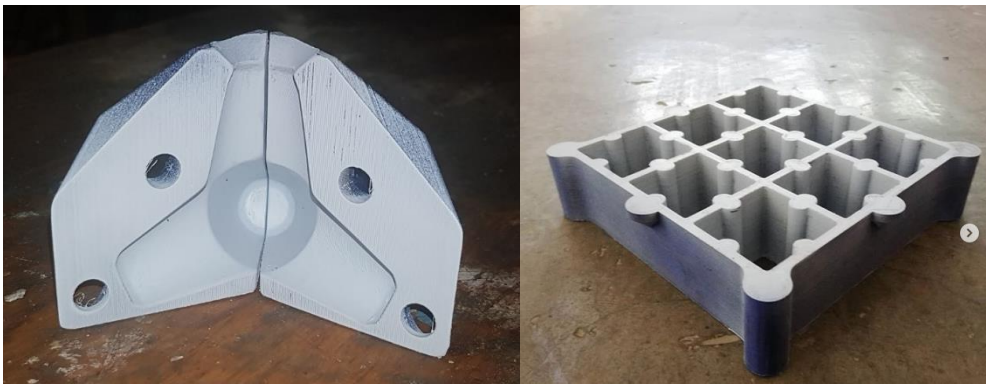

Figure 4.9: Mold of the tetrapod and antifer units

To have mass production, molds of antifer and tetrapod units should be increased while considering time limitations. In Figure 4.10, the mass production of tetrapod units and their molds could be seen.

Figure 4.10: Example tetrapod units used in the experiments and their mold

The last one is the vibration process and curing. To obtain a homogeneous artificial unit, the plate under the artificial units was vibrated with continuous hitting of a rubber hammer for approximately 1-2 minutes. After this process, the concrete setting process last 6-8 hours. After the demolding of units, the curing process takes place. The units were kept in water for 7 days.

4.4.2 Packing density

The definition and detailed information about packing density was mentioned in Chapter 2.2 of this thesis. In this study, packing density is a crucial parameter since it affects the stability coefficient and indirectly the weight of the unit used in the armor layer. In order to use the correct packing density and to check it through the placement of antifer blocks, pasteboard of known lengths was prepared and the number of antifers that could fit into these dimensions was calculated. Accordingly, it was checked whether the desired packing density is provided in many different places and orientations on the layer during irregular placement. In order to differentiate damage and its location more easily for irregularly placed antifer units at the armor layer, the antifers were divided into four regions having nearly the same dimensions and painted in four different colors for CS-A. As for CS-B, the antifers were divided into five regions having nearly the same dimensions and painted in five different colors. The two pasteboards are used to control packing density. Their dimensions are 30*30 and 20*20. Firstly, the pasteboard having dimensions of 20*20 is used at least three times to control each colored region. After all the regions are checked, the pasteboard having dimensions of 30*30 is used randomly to control the packing density with different configurations. To controlled area mostly two different colored regions. If there is a place that is not provided the required packing density, the irregular placement of antifer blocks in this area and nearby areas has been changed until it is provided with the approximately desired packing density. This process is repeated at the installation of each wave set.

4.5 Measurements

Water surface differences, which result from generated waves in the channel, could be measured by using DHI-202 type 60 cm long 16 wave gauges simultaneously. The example of the used gauge was given in Figure 4.11. The frequency of wave gauges was determined as 20 Hertz.

Figure 4.11: DHI-202 type 60 cm long wave gauge

4.5.1 Wave overtopping discharge measurements

Wave overtopping discharge measurements were done for the wave conditions (D1, D2, D3, D4-1, D4-2, and D5) given in Table 2.3, respectively. Wave overtopping was measured by using a 25 cm wide gutter plate and a collection chamber placed behind the gutter. The point at which the overtopped waves will gather is shown in Figure 4.12. At the end of each irregular wave series, by weighing the amount of water collected through the gutter, the average overtopping per unit length ($m^3/s/m$) was determined. The determined overtopping was then converted to a prototype scale. All dimensions given in the figure are in centimeters. The location of the gutter placed for overtopping measurements is indicated as the red line in the figure.

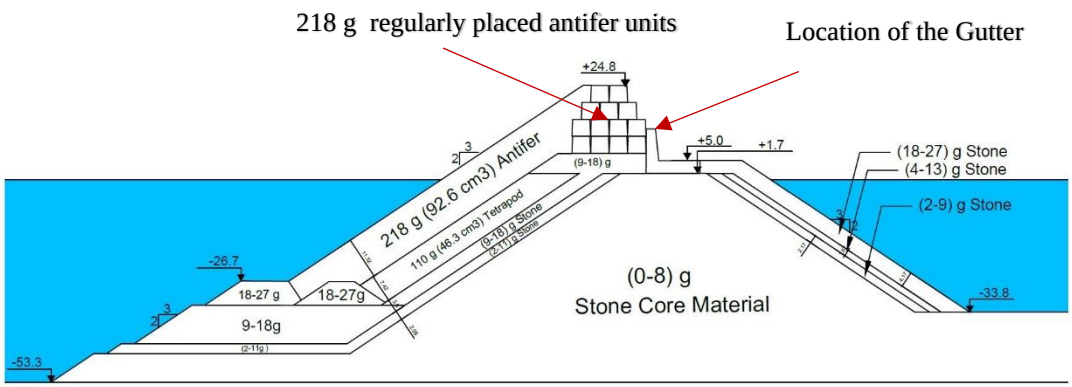

Figure 4.12: An example of the studied cross-section in the model scale.

4.5.2 Structural damage measurements/observations

Damage to the rubble mound breakwater armor layer is measured by considering the eroded area around the water level. However, in cases where artificial concrete blocks are used in the armor layer, it is recommended to define damage in terms of displaced blocks instead of making damage profile measurements (Van der Meer, 2017).

The damage in the breakwater armor layer is given in terms of N_{od}. The damage definition could be expressed based on the dislocated stones, as when a stone or artificial unit's movement is greater than its D_{n50}. That definition could be identified as damage to both the armor layer and toe (Van der Meer, 2017).

Experiments were recorded via video camera and photographed at an angle perpendicular to the cross-section. With the observations made through these videos and photographs, antifer units that have been rocking, or displaced units have been identified and their numbers and displacements have been reported. In addition, artificial units and natural stones, which were displaced in different alternative studies on the toe, were counted and their damage levels were determined. In the tests performed with artificial blocks, the measured damage amounts for each test set were calculated with the equations given below (4.3) and (4.3) separately for both the armor layer and the toe:

$$N_{od} = \frac{N_{s,armor\ layer}\ D_{n50,antifer}}{\mathrm{B}} \tag{4.2}$$

$$N_{od,toe} = \frac{N_{s,toe}\ D_{n50,toe}}{\mathrm{B}} \tag{4.3}$$

In the formula given above, the dimensionless displaced stone parameter is shown as $N_{od,\ armor}$ for the armor layer, $N_{s,armor\ layer}$ is the total number of antifers displaced in the armor layer at the end of a wave set, $D_{n50,antifer}$ is the nominal unit diameter of the antifer blocks used in the experiments. The dimensionless displaced stone parameter for the toe layer is given as $N_{od,\ toe}$, $N_{s,toe}$ is the total number of toe

stones displaced after the toe D1-D5 waves, and $D_{n50,\ the\ toe}$ represents the nominal grain diameters of the toe stones used in the toe experiments, and the width of the *B* section in the model scale. If the N_{od} value is between 0.2-0.5, it indicates initial level damage, between 0.5-1.5 indicates medium level damage, and greater than 2 and 2 indicates full damage level (Van der Meer, 2017).

4.5.3 Rear side structural damage measurements/observations

In the present study, the damage caused by wave overtopping on the rear side of the breakwater is expressed with the *S* parameter, which is given as a formula in the Equation (4.4), when natural rocks are used. If the *S* parameter is less than 2, it indicates initial level damage, between 3-5 indicates medium damage, and greater than 8 indicates full damage (Van der Meer, 2017).

$$S = \frac{Ae}{D_{n50}^2} \tag{4.4}$$

where *Ae* is eroded area and D_{n50} is the nominal diameter of the stone.

2-4 tons of stones were used on the existing rear side of CS-B. It was predicted that these stones could be damaged due to the waves breaking over the breakwater and experiments were carried out using 4-6 tons of stones instead of 2-4 tons of stones. For this reason, in the selected experiments, profile measurements were taken along the rear side and damage analysis was performed. The damage to the rear side armor layer was measured with a computer-controlled surface measurement system. The measuring system takes precise vertical distance measurements at desired intervals in both horizontal directions in an area of 1.5 m x 3.0 m. Banner® brand LTF24IC2LDQ model laser sensor was used for distance measurement in the measurement system. The vertical measurement accuracy of the system is below 0.3 mm, and the horizontal positioning accuracy is below 1.0 mm. With the surface measurement system, profile measurement was carried out along 8 different lines selected along the width of the channel before and after the experiment. Each profile

measurement was made from the midpoint of the crest to the rear side (in the direction of the length of the channel). With the help of the measured profiles, the extent of the damage on the rear side was determined Profile measurements were continued until the distances where morphological changes in the back area decreased and were thought to reach negligible levels. In order not to affect the measurement results of the canal walls, measurements were carried out in the region that is 16 cm away from each of the walls (in the direction of the width of the canal), and the transverse distance between the successive profiles (in the direction of the width of the canal) was determined as 8 cm. Thus, the damage on the rear side of the breakwater section could be measured in detail. In each of the profile measurements carried out, the distance between two-point measurements was determined as Δx=0.01 m. Comparisons of profile measurements before the experiment (before the D1 wave series) and after the experiment (after the D5 wave series) are given for each tested cross-section in the following sections of the study.

An example of profile measurements performed for CS-B-3 is presented in Figure 4.13. Vertical and horizontal axes are given as dimensionless in this example figure and the figures show the profile measurements will be given in the following part of the study. The vertical axis (y-axis) is the ratio of the average depth to the average grain diameter (D_{n50}) of the stone used in the harbor side armor layer of the breakwater; the horizontal axis (x-axis) is given as the ratio of the length from the back of the crest to the end of the section on the rear side with the average grain diameter of the stones used in the armor layer of the rear side of the breakwater.

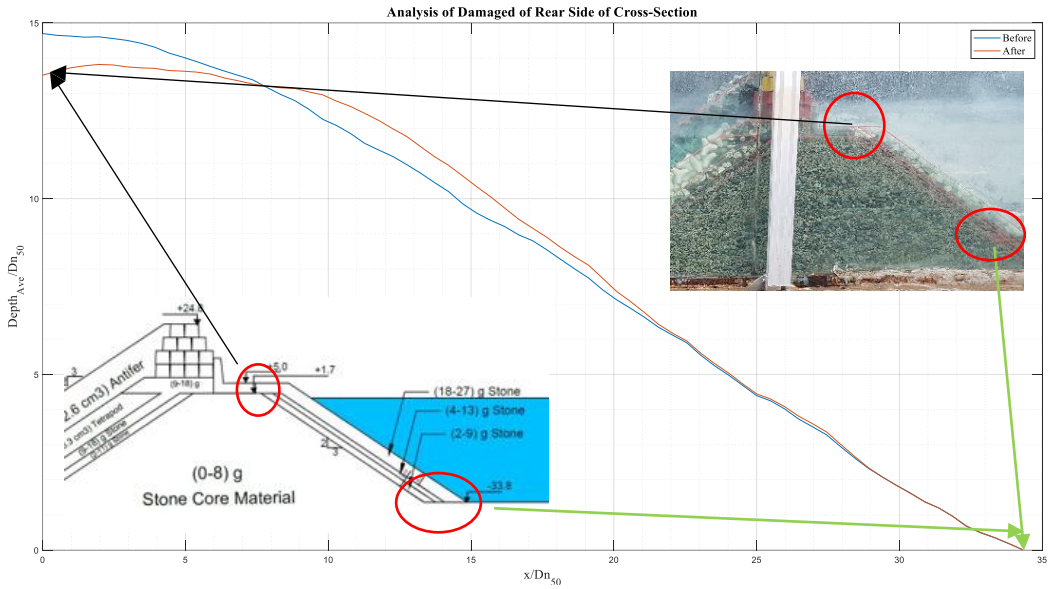

Figure 4.13: Laser measurement of rear side damage in CS-B-3

In the upper right photograph of Figure 4.13, the black line shows the first point of the profile measurement, and the green line shows the end point of the measurement. Based on the exemplified measurements above, the damage level was calculated by Equation (4.4).

4.6 Experimental program

In this physical model experiments, damage on the armor layer consisted of antifer units and toe consisted of both rock material and concrete cubes, and damage on the rear side resulting from wave overtopping was investigated. Furthermore, by changing the placement of antifer blocks on the crest of the breakwater, the effect on wave overtopping and damage was investigated. A total of 12 experiments were done. Four of them were done for the shallower section (CS-A) with two repetitions of each and, eight experiments were done for the deeper section (CS-B) with one repetition since the damage to the armor layer and toe was not acceptable except first and last experiments, which have two repetitions.

Table 4.5, it is given that indicating in which experiments the wave properties, seaside damage, rear side damage, and wave overtopping are measured. Also, the number of repetitions is given in Table 4.5. The significant changes for all alternatives were toe stone weight and water depth in front of the toe, and these differences will be discussed in Chapter 5.

Table 4.5: Summary of the test program.

Experiments		**Measurements**			
Cross-Section Name	**Number of repetitions**	**Wave**	**Seaside Damage**	**Rear Side Damage**	**Wave Overtopping**
CS-A-1	2	✓	✓	×	✓
CS-A-2	2	✓	✓	×	✓
CS-A-3	2	✓	✓	×	✓
CS-A-4	2	✓	✓	×	✓
CS-B-1	2	✓	✓	✓	×
CS-B-2	1	✓	✓	✓	×
CS-B-3	1	✓	✓	×	×
CS-B-4	1	✓	✓	✓	×
CS-B-5	1	✓	✓	×	×
CS-B-6	1	✓	✓	✓	×
CS-B-7	1	✓	✓	✓	×
CS-B-8	2	✓	✓	✓	✓

CHAPTER 5

RESULTS

The result part could be divided into two main parts. The first part is experimental results for CS-A, and the second part is experimental results for CS-B.

5.1 Experimental results for CS-A

Four experiments were conducted in the case of CS-A (Section 4-4). The results of these experiments were given in detail in related figures and tables.

5.1.1 Wave measurements

For each experiment, wave measurement and reflection analysis were done. For CS-A, one example of target and measured wave parameters was given in Table 5.1 for each wave condition.

Table 5.1:Measured and targeted wave characteristics for related wave conditions (given in model scale).

Wave Condition	Target		Measured (Set-1)		Measured (Set-2)	
	H_{m0} (m)	$T_{m-1.0}$ (s)	H_{m0} (m)	$T_{m-1.0}$ (s)	H_{m0} (m)	$T_{m-1.0}$ (s)
D1	0.09	1.222	0.086	1.248	0.087	1.251
D2	0.115	1.302	0.121	1.312	0.122	1.313
D3	0.135	1.417	0.138	1.43	0.138	1.432
D4-1	0.143	1.453	0.152	1.468	0.151	1.469
D4-2	0.143	1.453	0.149	1.472	0.149	1.47
D5	0.153	1.515	0.155	1.517	0.154	1.513

For all experiments, each measured wave parameters were nearly identical. Therefore, related wave parameters for each experiment will not be given.

5.1.2 Damage and wave overtopping measurements

Damage to the armor layer and toe could be indicated if a stone or artificial unit movement is greater than its D_{n50} (Van der Meer, 2017), as indicated in Section 4. With the use of a video recorder and before-and-after images of each experiment, the damage measurement is done. There was no repairment between the wave conditions until a new wave set was applied while calculating damage to the toe and armor layer.

For CS-A, four alternatives were tested, and the overtopping measurements and damage results of these alternatives were shown given in the below tables. The cross-section of each experiment was shown separately in the related figures below.

Physical model experiments were performed for CS-A, under wave and water level conditions specified in Table 4.4, the overtopping measurements for all cases were given in

Table 5.10, and damage results were given in Table 5.11. CS-A-1 is given at the prototype scale in Figure 5.1 and the red line indicates the location of the gutter used for overtopping measurements. All dimensions given in the figure are in meters.

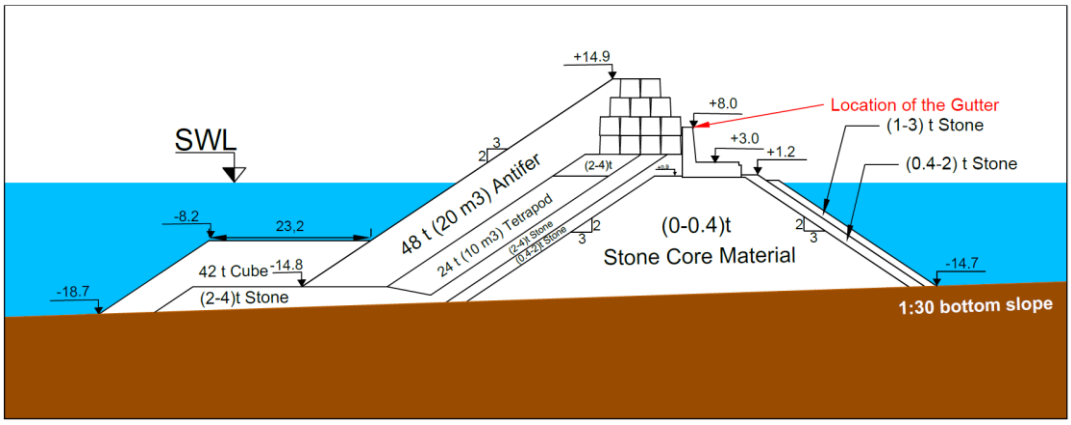

Figure 5.1: CS-A-1 in the prototype scale.

This alternative could be described as follows. 2-4 tons of stone to the bottom layer on the toe consisting of 42-ton cubes. In the case of the toe layer, two rows of 42-ton cubes are used. In the armor layer, 48-ton antifer blocks were placed irregularly with a 0.61 packing density. At the crest level of the armor layer, the placement of 48-ton antifer units was changed into a regular placement which takes place of a new crown wall.

In this study, all wave overtopping measurement table for each alternative cross-section includes wave series duration and measured wave overtopping at model scale and their equivalent values given at prototype scale. For CS-A-1, measured wave overtopping discharges are given in Table 5.2 for two sets at both model and prototype scales.

Table 5.2: Wave overtopping measurements in Set-1 and Set-2 of CS-A-1 for model and prototype scale.

CS-A-1		**Wave Set #**											
		Set # 1						**Set # 2**					
		D1	**D2**	**D3**	**D4-1**	**D4-2**	**D5**	**D1**	**D2**	**D3**	**D4-1**	**D4-2**	**D5**
Model	**Wave Series Duration (sec)**	2882	3772	4785	4888	4888	4849	2882	3772	4785	4888	4888	4849
	Measured Wave Overtopping (l)	0	0,51	9,13	17,91	31,58	60,00	0	0,54	10,29	20,55	36,82	58,00
	Wave Overtopping Discharge, q (l/s/m)	0,0000	0,0005	0,0076	0,0147	0,0258	0,0495	0,0000	0,0006	0,0086	0,0168	0,0301	0,0478
Prototype	**Wave Series Duration (hour)**	6,2	8,1	10,3	10,5	10,5	10,4	6,2	8,1	10,3	10,5	10,5	10,4
	Wave Overtopping Discharge, q (l/s/m)	**0,0**	**0,3**	**3,5**	**6,8**	**12,0**	**23,0**	**0,0**	**0,3**	**4,0**	**7,8**	**14,0**	**22,2**

In Table 5.2, the measured highest amount of wave overtopping is 0.0495 l/s/m (Wave Set 1) and 0.0478 l/s/m (Wave Set 2) at the HWL for the D5 wave condition in the model scale. These measurements correspond to 23.0 l/s/m and 22.2 l/s/m at the prototype scale, respectively.

The damage results calculated for the toe and the armor layer are grouped and given in Table 5.3. In this study, all damage measurement tables for each alternative cross-section, and the number of different colored antifer units that were displaced and rocking during the application of each wave condition in the armor layer and toe later are given. Maximum N_{od} values for CS-A-1 were found as 0.17 for the armor layer and 0.60 for the toe.

Table 5.3:Toe and armor layer damage measurements in Set-1 and Set-2 of CS-A-1

CS-A-1		Wave Set #													
		Set # 1							Set # 2						
		D1	D2	D3	D4-1	D4-2	D5	Σ	D1	D2	D3	D4-1	D4-2	D5	Σ
Armor Layer	# of Moved Units (Black)	0	0	0	0	0	0	0	0	0	0	0	0	0	0
	# of Moved Units (Green)	0	0	0	1	0	0	1	0	0	0	0	0	1	1
	# of Moved Units (Blue)	0	0	0	1	0	1	2	0	0	0	1	1	0	2
	# of Moved Units (Pink)	0	0	0	0	0	0	0	0	0	0	0	0	0	0
	# of Rocking Units	3	3	6	4	8	8	32	2	3	6	3	1	2	17
	N_{od}	**0.00**	**0.00**	**0.00**	**0.11**	**0.00**	**0.06**	**0.17**	**0.00**	**0.00**	**0.00**	**0.06**	**0.06**	**0.06**	**0.17**
	Cumulative N_{od}	**0.00**	**0.00**	**0.00**	**0.11**	**0.11**	**0.17**		**0.00**	**0.00**	**0.00**	**0.06**	**0.11**	**0.17**	
Toe	# of Moved Units	0	1	3	2	2	3	11	0	0	6	0	0	1	7
	# of Rocking Units	1	1	2	3	2	0	9	4	4	3	5	6	2	24
	$N_{od.\,t}$	**0.00**	**0.05**	**0.16**	**0.11**	**0.11**	**0.16**	**0.60**	**0.00**	**0.00**	**0.32**	**0.00**	**0.00**	**0.05**	**0.38**
	Cumulative $N_{od.\,t}$	**0.00**	**0.05**	**0.22**	**0.32**	**0.43**	**0.60**		**0.00**	**0.00**	**0.32**	**0.32**	**0.32**	**0.38**	

CS-A-2 was given at the prototype scale in Figure 5.2 and also red line indicates the location of the gutter used for overtopping measurements. All dimensions given in the figure are in meters.

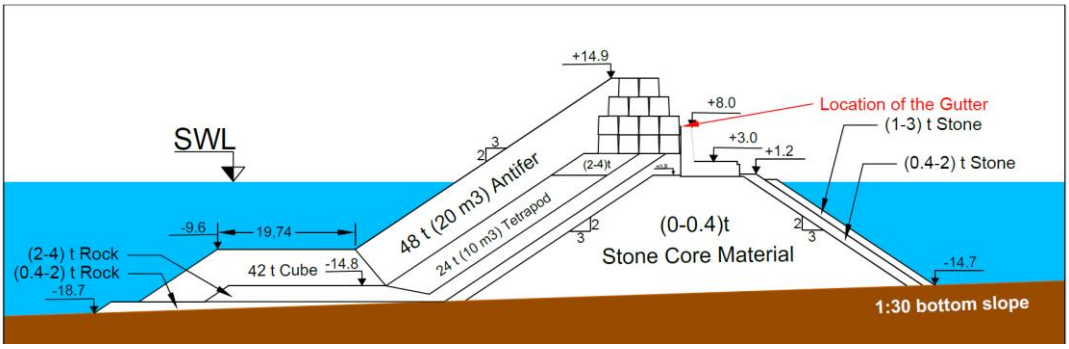

Figure 5.2: CS-A-2 in the prototype scale.

The differences between CS-A-1 and CS-A-2 are that the upper elevation of the toe is lowered from 8.2 meters to 9.6 meters. Furthermore, below the toe, 0.4-1-ton stones were placed to increase the stability of the toe. The armor layer was leaned to the toe. For CS-A-2, measured wave overtopping discharges are given in Table 5.4 for two sets at both model and prototype scales.

Table 5.4: Wave overtopping measurements in Set-1 and Set-2 of CS-A-2 for model and prototype scale.

CS-A-2		**Wave Set #**											
		Set # 1						**Set # 2**					
		D1	**D2**	**D3**	**D4-1**	**D4-2**	**D5**	**D1**	**D2**	**D3**	**D4-1**	**D4-2**	**D5**
Model	**Wave Series Duration (sec)**	2882	3772	4785	4888	4888	4849	2882	3772	4785	4888	4888	4849
	Measured Wave Overtopping (l)	0	4.7	28.28	46.53	64.01	97.43	0	2.45	13.2	27.14	40.89	72.56
	Wave Overtopping Discharge. q (l/s/m)	0.0000	0.0050	0.0236	0.0381	0.0524	0.0804	0.0000	0.0026	0.0110	0.0222	0.0335	0.0599
Prototype	**Wave Series Duration (hour)**	6.2	8.1	10.3	10.5	10.5	10.4	6.2	8.1	10.3	10.5	10.5	10.4
	Wave Overtopping Discharge. q (l/s/m)	**0.0**	**2.3**	**11.0**	**17.7**	**24.3**	**37.4**	**0.0**	**1.2**	**5.1**	**10.3**	**15.6**	**27.8**

In Table 5.4, the measured highest amount of wave overtopping is 0.0804 l/s/m (Wave Set 1) and 0.0599 l/s/m (Wave Set 2) at the HWL for the D5 wave condition in the model scale. These measurements correspond to 37.4 l/s/m and 27.8 l/s/m at the prototype scale, respectively. In this cross-section, the average wave overtopping at the HWL for the D5 wave condition was 32.6 l/s/m with a maximum of 37.4 l/s/m.

Although an increase was observed in the armor layer damage compared to the previous cross-section, the toe damage decreased. Damage in the armor layer was still below 0.5.

Table 5.5 shows the cumulative damage amounts for each wave condition in N_{od}, depending on the number of displaced units for CS-A-4 and, the maximum N_{od} for armor layer and toe found as 0.40 and 0.27, respectively.

Table 5.5:Toe and armor layer damage measurements in Set-1 and Set-2 of CS-A-2

CS-A-2		Wave Set #													
		Set # 1							Set # 2						
		D1	D2	D3	D4-1	D4-2	D5	Σ	D1	D2	D3	D4-1	D4-2	D5	Σ
Armor Layer	# of Moved Units (Black)	0	0	0	0	1	0	1	0	0	0	0	0	0	0
	# of Moved Units (Green)	0	0	0	0	0	0	0	0	0	0	0	1	0	1
	# of Moved Units (Blue)	0	1	0	0	3	0	4	0	1	0	0	1	0	2
	# of Moved Units (Pink)	0	0	0	0	2	0	2	0	0	1	0	0	0	1
	# of Rocking Units	6	6	8	15	12	13	60	8	17	9	17	11	9	71
	N_{od}	**0.00**	**0.06**	**0.00**	**0.00**	**0.34**	**0.00**	**0.40**	**0.00**	**0.06**	**0.06**	**0.00**	**0.11**	**0.00**	**0.23**
	Cumulative N_{od}	**0.00**	**0.06**	**0.06**	**0.06**	**0.40**	**0.40**		**0.00**	**0.06**	**0.11**	**0.11**	**0.23**	**0.23**	
Toe	# of Moved Units	0	0	1	0	0	3	4	0	0	1	2	0	2	5
	# of Rocking Units	2	4	4	2	0	1	13	4	2	7	0	2	2	17
	$N_{od.\ t}$	**0.00**	**0.00**	**0.05**	**0.00**	**0.00**	**0.16**	**0.22**	**0.00**	**0.00**	**0.05**	**0.11**	**0.00**	**0.11**	**0.27**
	Cumulative $N_{od.\ t}$	**0.00**	**0.00**	**0.05**	**0.05**	**0.05**	**0.22**		**0.00**	**0.00**	**0.05**	**0.16**	**0.16**	**0.27**	

CS-A-3 was given at the prototype scale in Figure 5.3 and also red line indicates the location of the gutter used for overtopping measurements. All dimensions given in the figure are in meters. Experiments for the first 2 alternative sections have shown that the armor layer and toe in these sections have high stability to wave conditions. Therefore, to reduce the section cost and to provide ease of manufacture, a different toe was designed by placing 4-6 tons of stones instead of 42-ton cubes 14 meters below sea level, with a toe width of 3 stones. It is also planned to place 0.4-1- and 0-0.4-ton stones under the 4–6-ton stones in the toe.

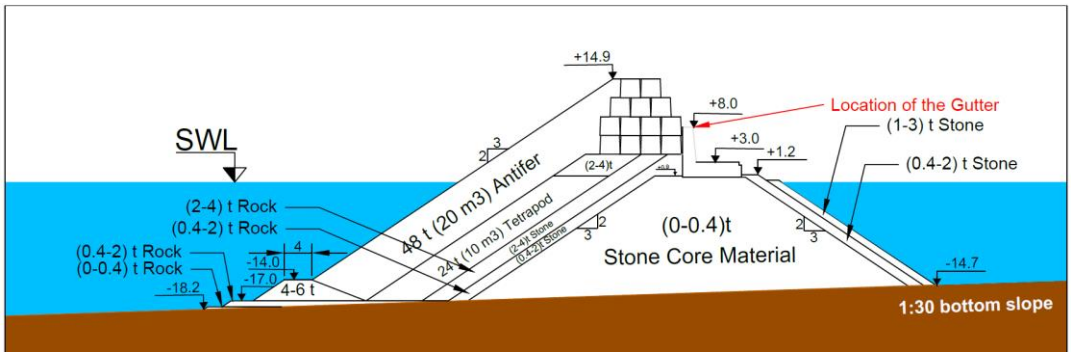

Figure 5.3: CS-A-3 in the prototype scale.

For CS-A-3, measured wave overtopping discharges are given in Table 5.6 for two sets at both model and prototype scales.

Table 5.6: Wave overtopping measurements in Set-1 and Set-2 of CS-A-3 for model and prototype scale.

CS-A-3		Wave Set #											
		Set # 1						Set # 2					
		D1	D2	D3	D4-1	D4-2	D5	D1	D2	D3	D4-1	D4-2	D5
Model	Wave Series Duration (sec)	2882	3772	4785	4888	4888	4849	2882	3772	4785	4888	4888	4849
	Measured Wave Overtopping (l)	0.04	8.83	41.77	65.78	93.22	123.99	0.00	6.63	42.01	83.91	115.02	158.83
	Wave Overtopping Discharge. q (l/s/m)	0.0001	0.0094	0.0349	0.0538	0.0763	0.1023	0.0000	0.0070	0.0351	0.0687	0.0941	0.1310
Prototype	Wave Series Duration (hour)	6.2	8.1	10.3	10.5	10.5	10.4	6.2	8.1	10.3	10.5	10.5	10.4
	Wave Overtopping Discharge. q (l/s/m)	**0.0**	**4.4**	**16.2**	**25.0**	**35.5**	**47.5**	**0.0**	**3.3**	**16.3**	**31.9**	**43.7**	**60.9**

In Table 5.6, the measured highest amount of wave overtopping is 0.1023 l/s/m (Wave Set 1) and 0.1310 l/s/m (Wave Set 2) at the HWL for the D5 wave condition in the model scale. These measurements correspond to 47.5 l/s/m and 60.9 l/s/m at the prototype scale, respectively. In this cross-section, the average wave overtopping at the HWL for the D5 wave condition was 54.2 l/s/m with a maximum of 60.9 l/s/m.

Table 5.7 shows the cumulative damage amounts for each wave condition in N_{od}, depending on the number of displaced units for CS-A-3 and, the maximum N_{od} for armor layer and toe found as 0.51 and 1.07, respectively. Damage in the armor layer was still below 0.5. An increase in damage was observed in both the toe and the armor layer. The damage measurement obtained for the armor layer was at the initial limit, and the damage measurement obtained for the toe was above the acceptable level.

Table 5.7: Toe and armor layer damage measurements in Set 1 and Set-2 of CS-A-3

CS-A-3		Wave Set #													
		Set # 1							Set # 2						
		D1	**D2**	**D3**	**D4-1**	**D4-2**	**D5**	**Σ**	**D1**	**D2**	**D3**	**D4-1**	**D4-2**	**D5**	**Σ**
Armor Layer	**# of Moved Units (Black)**	0	0	0	0	0	0	0	0	0	0	0	0	0	0
	# of Moved Units (Green)	1	0	1	0	1	0	3	0	0	0	0	0	0	0
	# of Moved Units (Blue)	0	0	0	0	1	1	2	0	0	0	0	0	0	0
	# of Moved Units (Pink)	1	2	1	0	0	0	4	0	3	5	0	1	0	9
	# of Rocking Units	0	6	3	9	4	2	24	2	3	1	3	3	1	13
	N_{od}	**0.11**	**0.11**	**0.11**	**0.00**	**0.11**	**0.06**	**0.51**	**0.00**	**0.17**	**0.28**	**0.00**	**0.06**	**0.00**	**0.51**
	Cumulative N_{od}	**0.11**	**0.23**	**0.34**	**0.34**	**0.45**	**0.51**		**0.00**	**0.17**	**0.45**	**0.45**	**0.51**	**0.51**	
Toe	**# of Moved Units**	1	11	11	10	3	5	41	3	12	10	6	5	6	42
	# of Rocking Units	0	0	1	0	0	0	1	0	0	0	0	0	0	0
	$N_{od.\,t}$	**0.03**	**0.28**	**0.28**	**0.26**	**0.08**	**0.13**	**1.05**	**0.08**	**0.31**	**0.26**	**0.15**	**0.13**	**0.15**	**1.07**
	Cumulative $N_{od.\,t}$	**0.03**	**0.31**	**0.59**	**0.84**	**0.92**	**1.05**		**0.08**	**0.38**	**0.64**	**0.79**	**0.92**	**1.07**	

CS-A-4 was given at the prototype scale in Figure 5.4 and also red line indicates the location of the gutter used for overtopping measurements. All dimensions given in the figure are in meters. In the CS-A-4, the toe height has been increased from 14.0 m below the still water level to 13.7 m below the still water level in order to increase the support of the antifer blocks from the toe and to reduce the wave overtopping. Thus, to decrease an expected increase in damage and to improve the stability of the toe, the toe width has been doubled.

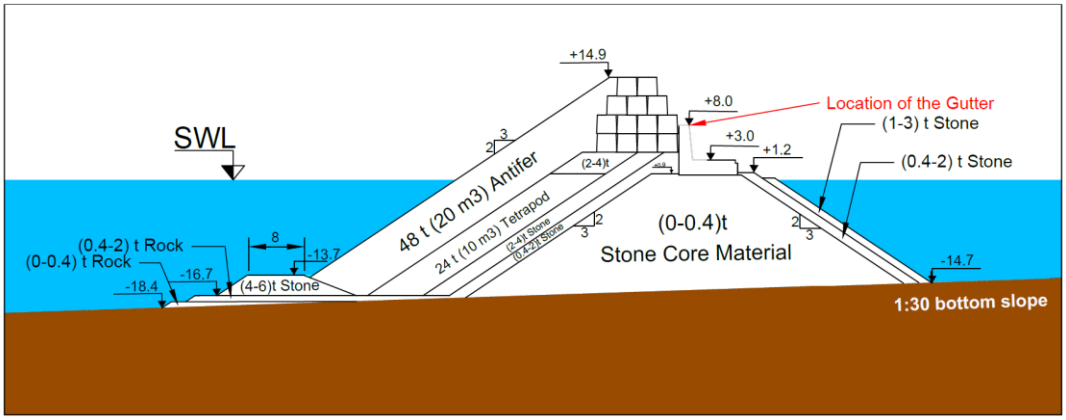

Figure 5.4: CS-A-4 in the prototype scale.

For CS-A-4, measured wave overtopping discharges are given Table 5.8 for two sets at both model and prototype scales.

Table 5.8: Wave overtopping measurements in Set-1 and Set-2 of CS-A-4 for model and prototype scale.

CS-A-4		Wave Set #											
		Set # 1						Set # 2					
		D1	D2	D3	D4-1	D4-2	D5	D1	D2	D3	D4-1	D4-2	D5
Model	Wave Series Duration (sec)	2882	3772	4785	4888	4888	4849	2882	3772	4785	4888	4888	4849
	Measured Wave Overtopping (l)	0.02	2.99	24.48	46.59	62.38	80.34	0	4.04	26.91	75.87	114.75	127.10
	Wave Overtopping Discharge. q (l/s/m)	0.0000	0.0032	0.0205	0.0381	0.0510	0.0663	0.0000	0.0043	0.0225	0.0621	0.0939	0.1048
Prototype	Wave Series Duration (hour)	6.2	8.1	10.3	10.5	10.5	10.4	6.2	8.1	10.3	10.5	10.5	10.4
	Wave Overtopping Discharge. q (l/s/m)	**0.0**	**1.5**	**9.5**	**17.7**	**23.7**	**30.8**	**0.0**	**2.0**	**10.5**	**28.9**	**43.6**	**48.7**

The measured highest amount of wave overtopping is 0.0663 l/s/m (Wave Set 1) and 0.1048 l/s/m (Wave Set 2) at the HWL for the D5 wave condition in the model scale.

These measurements correspond to 30.8 l/s/m and 48.7 l/s/m at the prototype scale, respectively. In this cross-section, the average wave overtopping at the HWL for the D5 wave condition was 39.8 l/s/m with a maximum of 48.7 l/s/m.

There was no change in armor layer damage but an increase in toe damage was observed. The damage measurement obtained for the armor layer was at the initial limit, and the damage measurement obtained for the toe was above the initial level. Table 5.9 shows the cumulative damage amounts for each wave condition in N_{od}, depending on the number of displaced units for CS-A-4. For CS-A-4, maximum N_{od} for armor layer and toe found as 0.51 and 1.28, respectively. An increase was observed in the toe damage compared to the previous cross-section. Damage in the armor layer was still below the initial limit.

Table 5.9:Toe and armor layer damage measurements in Set-1 and Set-2 of CS-A-4

CS-A-4		**Wave Set #**													
		Set # 1							**Set # 2**						
		D1	**D2**	**D3**	**D4-1**	**D4-2**	**D5**	**Σ**	**D1**	**D2**	**D3**	**D4-1**	**D4-2**	**D5**	**Σ**
Armor Layer	**# of Moved Units (Black)**	0	0	0	0	0	0	0	0	0	0	0	0	0	2
	# of Moved Units (Green)	1	0	1	0	1	0	3	0	0	0	0	0	0	2
	# of Moved Units (Blue)	0	0	0	0	1	1	2	0	0	0	0	0	0	0
	# of Moved Units (Pink)	1	2	1	0	0	0	4	0	3	5	0	1	0	2
	# of Rocking Units	0	6	3	9	4	2	24	2	3	1	3	3	1	31
	N_{od}	**0.11**	**0.11**	**0.11**	**0.00**	**0.11**	**0.06**	**0.51**	**0.00**	**0.17**	**0.28**	**0.00**	**0.06**	**0.00**	**0.34**
	Cumulative N_{od}	**0.11**	**0.23**	**0.34**	**0.34**	**0.45**	**0.51**		**0.00**	**0.17**	**0.45**	**0.45**	**0.51**	**0.51**	
Toe	**# of Moved Units**	1	11	11	10	3	5	41	3	12	10	6	5	6	50
	# of Rocking Units	0	0	1	0	0	0	1	0	0	0	0	0	0	5
	$N_{od.\,t}$	**0.03**	**0.28**	**0.28**	**0.26**	**0.08**	**0.13**	**1.05**	**0.08**	**0.31**	**0.26**	**0.15**	**0.13**	**0.15**	**1.28**
	Cumulative $N_{od.\,t}$	**0.03**	**0.31**	**0.59**	**0.84**	**0.92**	**1.05**		**0.08**	**0.38**	**0.64**	**0.79**	**0.92**	**1.07**	

5.1.2.1 Summaries of experimental results

To have a better understanding of the alternative cross-sections, summary tables are given below. In

Table 5.10, wave overtopping summary tables is shown for two sets of each alternative cross-section in model and prototype scale. Wave overtopping is shown as 'Wave Over.', and the wave condition is shown as 'W. Cond.', Exceedance/Occurrence Probability is shown as 'Exc./Oc. P.', and the name of the alternative is expressed as 'ALT.'.

Table 5.10: The amount of wave overtopping measured in set-1 and wave set-2 of each experiment for CS-A (on both model and prototype scale).

Set #			Set # 1						Set # 2					
ALT. #	Wave Cond.		D1	D2	D3	D4-1	D4-2	D5	D1	D2	D3	D4-1	D4-2	D5
	Water Level		W1	W2	W2	W1	W3	W3	W1	W2	W2	W1	W3	W3
	Exc./ Occur. Prob.		*	**	***	****	****	*+	*	**	***	****	****	*+
CS-A-1	Wave Over. q (l/s/m)	M.	0.0000	0.0005	0.0076	0.0147	0.0258	0.0495	0.0000	0.0006	0.0086	0.0168	0.0301	0.0478
		Pro.	**0.0**	**0.3**	**3.5**	**6.8**	**12.0**	**23.0**	**0.0**	**0.3**	**4.0**	**7.8**	**14.0**	**22.2**
CS-A-2	Wave Over. q (l/s/m)	M.	0.0000	0.0050	0.0236	0.0381	0.0524	0.0804	0.0000	0.0026	0.0110	0.0222	0.0335	0.0599
		Pro.	**0.0**	**2.3**	**11.0**	**17.7**	**24.3**	**37.4**	**0.0**	**1.2**	**5.1**	**10.3**	**15.6**	**27.8**
CS-A-3	Wave Over. q (l/s/m)	M.	0.0001	0.0094	0.0349	0.0538	0.0763	0.1023	0.0000	0.0070	0.0351	0.0687	0.0941	0.1310
		Pro.	**0.0**	**4.4**	**16.2**	**25.0**	**35.5**	**47.5**	**0.0**	**3.3**	**16.3**	**31.9**	**43.7**	**60.9**
CS-A-4	Wave Over. q (l/s/m)	M.	0.0000	0.0032	0.0205	0.0381	0.0510	0.0663	0.0000	0.0043	0.0225	0.0621	0.0939	0.1048
		Pro.	**0.0**	**1.5**	**9.5**	**17.7**	**23.7**	**30.8**	**0.0**	**2.0**	**10.5**	**28.9**	**43.6**	**48.7**
*:10 hrs., **:5 yr., ***: 50yr., ****:100 yr., *+: 100 yr., upper limit (90%). W1: LWL, W2: MWL, W3: HWL														

In Table 5.11, measured damage to armor and toe layers is shown for two sets of each alternative cross-section. Similar abbreviations are used like in Table 5.10 , W. Cond. means wave conditions, Exc./Oc. P. means Exceedance/Occurrence Probability, A.L. means armor layer and ALT. means alternatives. Moreover, cumulative values are shown with the Σ sign.

Table 5.11: The amount of damage level measured in set 1 and wave set 2 of each experiment for CS-A.

Set #			Set # 1							Set # 2						
ALT.	**Part**	**Wave Cond.**	**D1**	**D2**	**D3**	**D4-1**	**D4-2**	**D5**	**Σ**	**D1**	**D2**	**D3**	**D4-1**	**D4-2**	**D5**	**Σ**
		Water Level	W1	W2	W2	W1	W3	W3		W1	W2	W2	W1	W3	W3	
		Exc./ Occur. Prob.	*	**	***	****	****	*+		*	**	***	****	****	*+	
CS-A-1	**A. L.**	**N_{od}**	0.00	0.00	0.00	0.11	0.00	0.06	**0.17**	0.00	0.00	0.00	0.06	0.06	0.06	**0.17**
		Σ N_{od}	0.00	0.00	0.00	0.11	0.11	0.17		0.00	0.00	0.00	0.06	0.11	0.17	
	Toe	**$N_{od.t}$**	0.00	0.05	0.16	0.11	0.11	0.16	**0.60**	0.00	0.00	0.32	0.00	0.00	0.05	**0.38**
		Σ $N_{od.t}$	0.00	0.05	0.22	0.32	0.43	0.60		0.00	0.00	0.32	0.32	0.32	0.38	
CS-A-2	**A. L.**	**N_{od}**	0.00	0.06	0.00	0.00	0.34	0.00	**0.40**	0.00	0.06	0.06	0.00	0.11	0.00	**0.23**
		Σ N_{od}	0.00	0.06	0.06	0.06	0.40	0.40		0.00	0.06	0.11	0.11	0.23	0.23	
	Toe	**$N_{od.t}$**	0.00	0.00	0.05	0.00	0.00	0.16	**0.22**	0.00	0.00	0.05	0.11	0.00	0.11	**0.27**
		Σ $N_{od.t}$	0.00	0.00	0.05	0.05	0.05	0.22		0.00	0.00	0.05	0.16	0.16	0.27	
CS-A-3	**A. L.**	**N_{od}**	0.11	0.11	0.11	0.00	0.11	0.06	**0.51**	0.00	0.17	0.28	0.00	0.06	0.00	**0.51**
		Σ N_{od}	0.11	0.23	0.34	0.34	0.45	0.51		0.00	0.17	0.45	0.45	0.51	0.51	
	Toe	**$N_{od.t}$**	0.03	0.28	0.28	0.26	0.08	0.13	**1.05**	0.08	0.31	0.26	0.15	0.13	0.15	**1.07**
		Σ $N_{od.t}$	0.03	0.31	0.59	0.84	0.92	1.05		0.08	0.38	0.64	0.79	0.92	1.07	
CS-A-4	**A. L.**	**N_{od}**	0.00	0.23	0.06	0.11	0.11	0.00	**0.51**	0.00	0.00	0.11	0.17	0.00	0.06	**0.34**
		Σ N_{od}	0.00	0.23	0.28	0.40	0.51	0.51		0.00	0.00	0.11	0.28	0.28	0.34	
	Toe	**$N_{od.t}$**	0.03	0.20	0.20	0.28	0.10	0.23	**1.05**	0.00	0.56	0.48	0.10	0.00	0.13	**1.28**
		Σ $N_{od.t}$	0.03	0.23	0.43	0.71	0.82	1.05		0.00	0.56	1.05	1.15	1.15	1.28	

*:10 hrs., **:5 yr., ***: 50yr., ****:100 yr., *+: 100 yr., upper limit (90%); W1: LWL, W2: MWL, W3: HWL

In Figure 5.5, all tested cross-sections are shown focusing on the main difference (toe) between each alternative. This figure is given as a summary of all the modifications in CS-A described above.

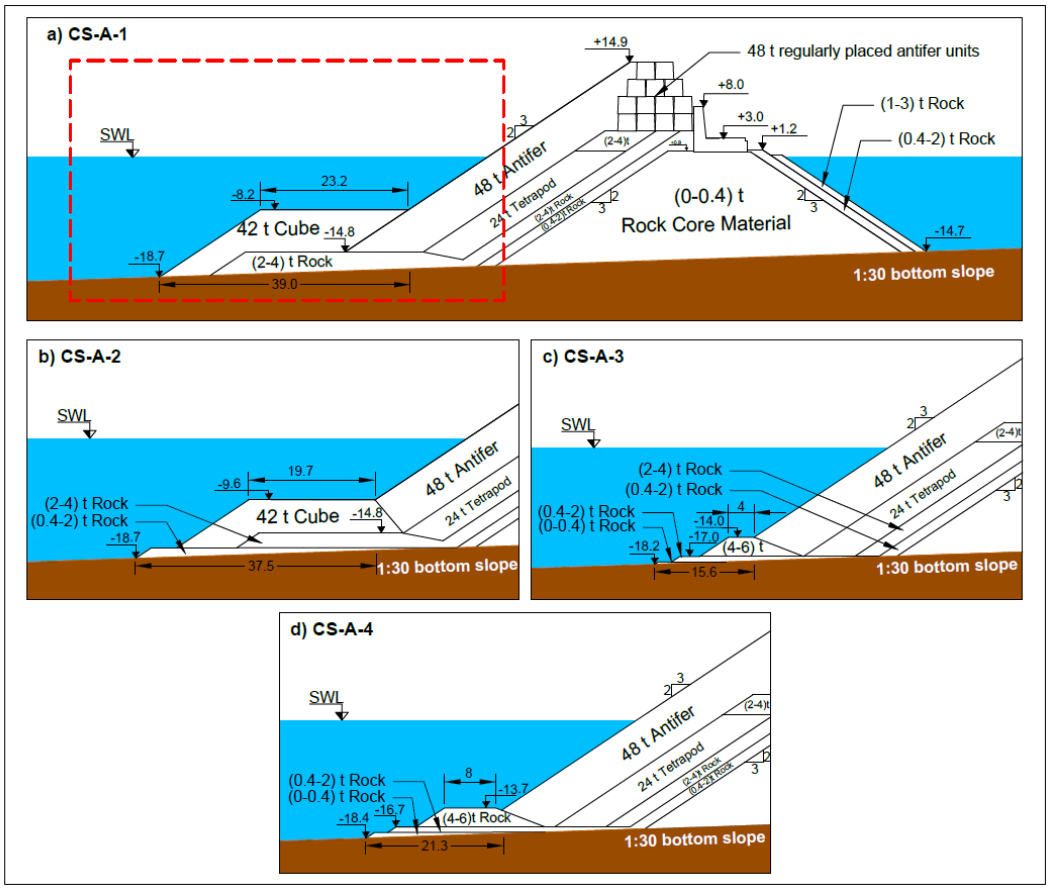

Figure 5.5: All tested cross-sections for CS-A at prototype scale (All dimensions given in the figure are in meters).

5.2 Experimental results for CS-B

In the case of CS-B, eight experiments were carried out. The outcomes of these tests were given in detail in the figures and tables below.

5.2.1 Wave measurements

Wave measurement and reflection analysis were performed for each experiment. Table 5.12 shows one illustration of the target and measured wave characteristics for each wave condition in CS-B. For all tests, each measured wave parameters were nearly indistinguishable. As a result, related wave parameters for each experiment will not be given.

Table 5.12: Measured and targeted wave characteristics for related wave conditions (given in model scale).

Wave Cond.	Target		Measured (Set-1)		Measured (Set-2)	
	H_{m0} (m)	$T_{m-1.0}$ (s)	H_{m0} (m)	$T_{m-1.0}$ (s)	H_{m0} (m)	$T_{m-1.0}$ (s)
D1	0.09	1.22	0.09	1.23	0.083	1.23
D2	0.115	1.30	0.114	1.30	0.114	1.30
D3	0.135	1.42	0.134	1.42	0.134	1.41
D4-1	0.143	1.45	0.143	1.45	0.142	1.45
D4-2	0.143	1.45	0.135	1.46	0.143	1.46
D5	0.153	1.52	0.146	1.51	0.153	1.51

5.2.2 Seaward side damage, rear side damage, and wave overtopping measurements

The same principles were applied for damage definition and overtopping measurements. However, to investigate the rear side damage, a laser meter was used. Some methodology used in CS-A is implemented. To measure surface profile, eight profile measurements were made from the midpoint of the crest to the back area (in the x-direction) before and after the experiment. With the help of the profiles, the length section information of the damages that will occur on the lee side has been obtained. Profile measurements were continued until the distances where morphological changes in the back area decreased and were thought to reach negligible levels. The distance between the profiles is eight centimeters. Profiles were taken from a distance of 16 cm from the channel walls. The distance between

two-point measurements in each profile (line) was determined as Δx=0.01 m. Comparative plots before and after the wave set (after the D5 wave series) are given for each alternative.

Physical model experiments were performed for CS-B, under wave and water level conditions specified in Table 4.4. For CS-B, eight alternatives were conducted, and the outcomes of these alternatives were given rear side damage results of alternatives were given in Table 5.22, and seaward side damage in Table 5.23. Each experiment's cross-section was shown separately in the figures given below. CS-B-1 was given at the prototype scale in Figure 5.6.

This alternative could be explained as 2-4 tons of stone were placed on the bottom layer on the toe consisting of 4-6-ton stones. 48-ton antifer blocks were placed irregularly with a 0.61 packing density on the existing 24-ton tetrapod artificial blocks with a slope of 3H:2V in the armor layer of the section. At the crest level of the armor layer, the placement of 48-ton antifer units was changed into a regular placement which takes place of a new crown wall. Behind the crest, 4–6-ton stones were used.

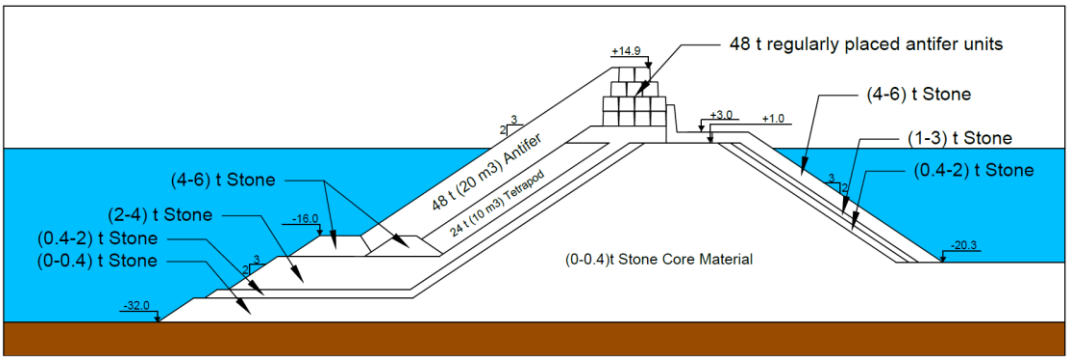

Figure 5.6: CS-B-1 in the prototype scale. (All dimensions given in the figure are in meters.)

Table 5.13 shows the cumulative damage amounts for each wave condition in N_{od}, depending on the number of displaced units for CS-B-1. For CS-B-1, maximum N_{od} for armor layer and toe found as 2.09 and 3.34 respectively.

Table 5.13: Toe and armor layer damage in Set-1 and Set-2 of CS-B-1

CS-B-1		Wave Set #													
		Set # 1							Set # 2						
		D1	**D2**	**D3**	**D4-1**	**D4-2**	**D5**	**Σ**	**D1**	**D2**	**D3**	**D4-1**	**D4-2**	**D5**	**Σ**
Armor Layer	**# of Moved Units (Grey)**	0	0	0	0	0	2	2	0	0	0	0	1	0	1
	# of Moved Units (Black)	0	0	0	0	1	1	2	0	0	0	0	1	0	1
	# of Moved Units Green)	0	0	0	1	0	1	2	0	0	2	1	0	1	4
	# of Moved Units (Blue)	0	0	2	2	0	0	4	0	0	1	2	1	1	5
	# of Moved Units (Pink)	1	5	12	8	1	0	27	3	4	12	2	2	0	23
	# of Rocking Units	4	14	5	9	15	12	59	6	16	12	9	8	14	65
	N_{od}	**0.06**	**0.28**	**0.79**	**0.62**	**0.11**	**0.23**	**2.09**	**0.17**	**0.23**	**0.85**	**0.28**	**0.28**	**0.11**	**1.92**
	Cumulative N_{od}	**0.06**	**0.34**	**1.13**	**1.75**	**1.86**	**2.09**		**0.17**	**0.40**	**1.24**	**1.53**	**1.81**	**1.92**	
Toe	**# of Moved Units**	1	16	11	29	11	6	74	1	10	45	41	19	15	131
	# of Rocking Units	0	7	4	12	4	7	34	2	14	8	7	12	3	46
	$N_{od.\ t}$	**0.03**	**0.41**	**0.28**	**0.74**	**0.28**	**0.15**	**1.89**	**0.03**	**0.26**	**1.15**	**1.05**	**0.48**	**0.38**	**3.34**
	Cumulative $N_{od.\ t}$	**0.03**	**0.43**	**0.71**	**1.45**	**1.73**	**1.89**		**0.03**	**0.28**	**1.43**	**2.47**	**2.96**	**3.34**	

An example figure of rear side damage measurements is shown in Figure 5.7. The damage level measurements of the rear side armor layer were calculated using profile measurements according to the differences between before the D1 wave condition and after the D5 wave condition. In this figure, the blue line shows the one profile of the rear side armor layer of the cross-section before the storm and the orange line shows the newly formed profile after the damage and accumulation caused by the wave overtopping at the end of one wave set. Maximum rear side damage S_{max} found as 10.3 and average rear side damage, S_{ave} for armor layer found as 6.0270.

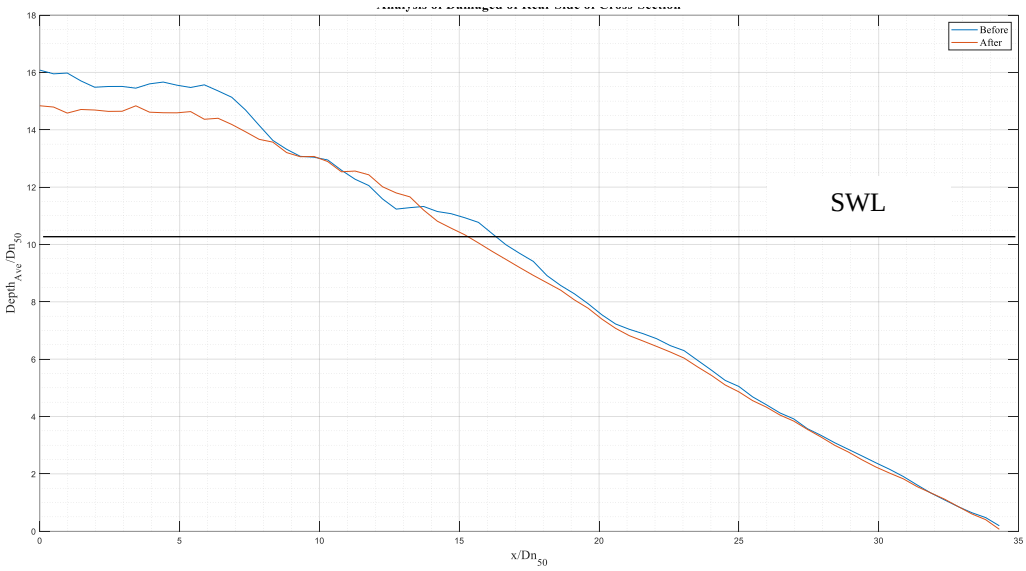

Figure 5.7:Rear side damage level profile measured by laser-meter for CS-B-1

It has been observed that the damage in the rear side armor layer of the breakwater is above the acceptable level (*S*=2). As a result of the tests carried out for CS-B-1, it was decided to make a revision in the section, considering the damage observed in the armor layers (sea and rear sides) and the toe.

For CS-B-2, the upper elevation of the toe remained the same as the previous cross-section, but the weight of stones in the toe changed from 4-6 tons to 6–8-ton stones. In this test, a discrepancy was observed between the design and the model due to the use of antifer blocks on the existing artificial units and toe in the cross-section resulting from irregular placement of antifers and existing toe. It has been discovered that the drawing limits can be complied with if antifer blocks are placed as a single layer in the vicinity of the existing toe in the armor layer. As a result, it started with a single row of antifers at the above toe and double rows of antifers were placed on the upper elevations of the armor layer. However, it was observed that placing one layer just above the toe results in exposure to the second layer of antifers, which increases the damage to the armor layer. CS-B-2 was given at the prototype scale in Figure 5.8.

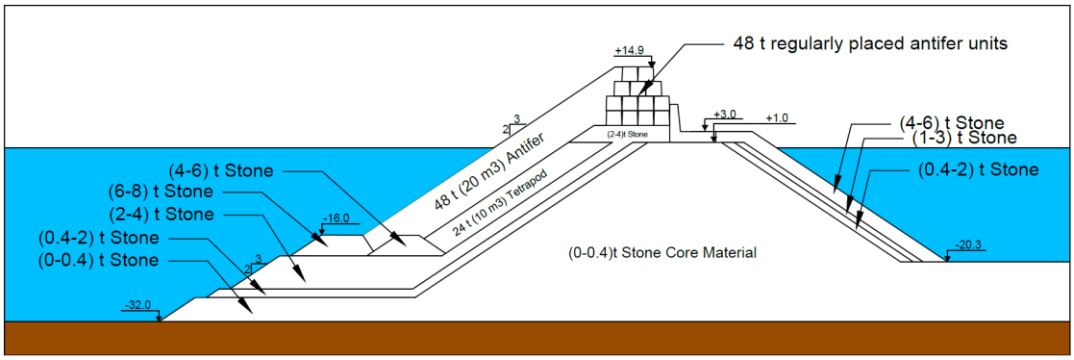

Figure 5.8: CS-B-2 in the prototype scale. (All dimensions given in the figure are in meters.)

Table 5.14 shows the cumulative damage amounts for each wave condition in N_{od}, depending on the number of displaced units for CS-B-2.

For CS-B-2, maximum N_{od} for armor layer and toe found as 1.02 and 2.52 respectively. Moreover, maximum rear side damage S_{max} found as 6.3 and average rear side damage, S_{ave} for armor layer found as 2.48. It has been observed that the damage in the rear side armor layer of the breakwater is above the acceptable level (S=2). As a result of the tests carried out for CS-B-2, it was decided to make a revision in the section, taking into account the damage observed in the armor layers (sea and rear sides) and the toe.

Table 5.14: Toe and armor layer damage measurements in CS-B-2

CS-B-2		Wave Set #						
		Set # 1						
		D1	**D2**	**D3**	**D4-1**	**D4-2**	**D5**	**Σ**
Armor Layer	**# of Moved Units (Grey)**	0	0	0	0	0	0	0
	# of Moved Units (Black)	0	0	0	0	0	0	0
	# of Moved Units (Green)	0	0	1	1	0	0	2
	# of Moved Units (Blue)	0	0	0	0	0	0	0
	# of Moved Units (Pink)	2	4	7	2	1	0	16
	# of Rocking Units	2	1	2	3	2	0	10
	N_{od}	**0.11**	**0.23**	**0.45**	**0.17**	**0.06**	**0.00**	**1.02**
	Cumulative N_{od}	**0.11**	**0.34**	**0.79**	**0.96**	**1.02**	**1.02**	
Toe	**# of Moved Units**	0	8	24	15	10	16	73
	# of Rocking Units	0	3	15	11	8	9	46
	$N_{od.\,t}$	**0.00**	**0.28**	**0.83**	**0.52**	**0.35**	**0.55**	**2.52**
	Cumulative $N_{od.\,t}$	**0.00**	**0.28**	**1.11**	**1.62**	**1.97**	**2.52**	

After this cross-section, CS-B-3 was experimented with just to solve the previous problem by placing at least 2 rows of antifer solutions applied for the armor layer up to the toe without considering the change in the slope of the layer. The damage to the armor layer had been lessened due to the solution. CS-B-3 was given at the prototype scale in Figure 5.9.

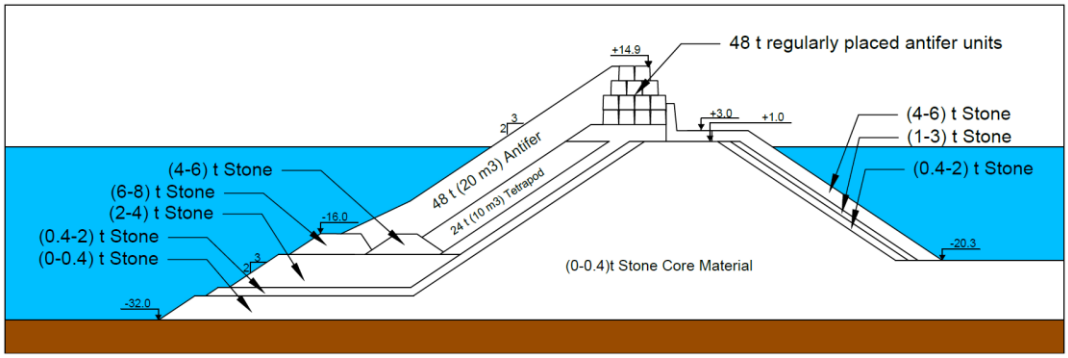

Figure 5.9: CS-B-3 in the prototype scale. (All dimensions given in the figure are in centimeters.)

Table 5.15 shows the cumulative damage amounts for each wave condition in N_{od}, depending on the number of displaced units for CS-B-3. Since this test was done to find a solution to the specific problem mentioned above, the rear side damage measurement was not done. For CS-B-3, although all wave sets were not implemented, for D4-1, D4-2, and D5 wave conditions, maximum N_{od} for armor layer and toe found as 0.28 and 1.11 respectively.

Table 5.15: Toe and armor layer damage measurements in CS-B-3

CS-B-3		Wave Set #						
		Set # 1						
		D1	D2	D3	D4-1	D4-2	D5	Σ
Armor Layer	# of Moved Units (Grey)	-	-	-	0	0	0	0
	# of Moved Units (Black)	-	-	-	1	1	0	2
	# of Moved Units (Green)	-	-	-	0	0	2	2
	# of Moved Units (Blue)	-	-	-	0	0	0	0
	# of Moved Units (Pink)	-	-	-	1	0	0	1
	# of Rocking Units	-	-	-	19	8	17	44
	N_{od}	-	-	-	**0.11**	**0.06**	**0.11**	**0.28**
	Cumulative N_{od}	-	-	-	**0.11**	**0.17**	**0.28**	
Toe	# of Moved Units	-	-	-	25	5	2	32
	# of Rocking Units	-	-	-	8	5	9	22
	$N_{od.\ t}$	-	-	-	**0.86**	**0.17**	**0.07**	**1.11**
	Cumulative $N_{od.\ t}$	-	-	-	**0.86**	**1.04**	**1.11**	

After resolving the issue regarding the prior cross-section, CS-B-4 was experimented with. In this test, the stone weight on the toe increased from 6-8-ton to 8-10-ton stone weight. In this cross-section, it was observed that damage to the toe had decreased. CS-B-4 was given at the prototype scale in Figure 5.10.

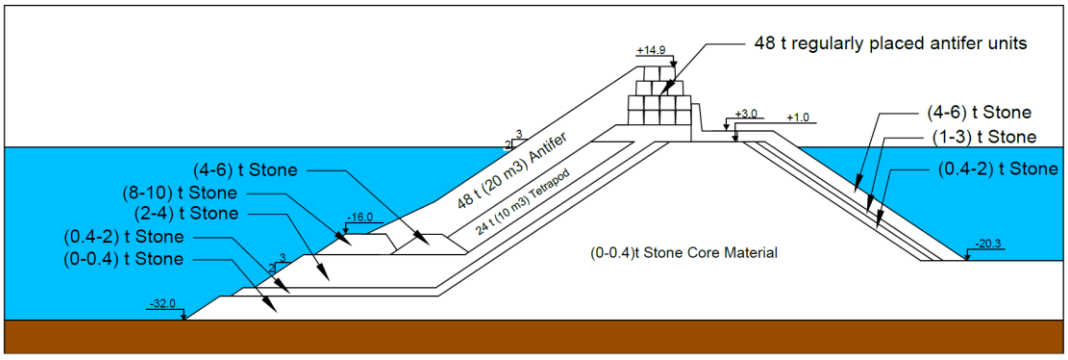

Figure 5.10: CS-B-4 in the prototype scale. (All dimensions given in the figure are in centimeters.)

Table 5.16 shows the cumulative damage amounts for each wave condition in N_{od}, depending on the number of displaced units for CS-B-4. Maximum N_{od} for armor layer and toe found as 0.06 and 0.86 respectively. Furthermore, maximum rear side damage S_{max} found as 0.9 and average rear side damage, S_{ave} for armor layer found as 0.3955.

Table 5.16: Toe and armor layer damage measurements in CS-B-4

CS-B-4		Wave Set #						
		Set # 1						
		D1	D2	D3	D4-1	D4-2	D5	Σ
Armor Layer	# of Moved Units (Grey)	0	0	0	0	1	0	1
	# of Moved Units (Black)	0	0	0	0	0	0	0
	# of Moved Units (Green)	0	0	0	0	0	0	0
	# of Moved Units (Blue)	0	0	0	0	0	0	0
	# of Moved Units (Pink)	0	0	0	0	0	0	0
	# of Rocking Units	6	12	7	2	1	6	34
	N_{od}	**0.00**	**0.00**	**0.00**	**0.00**	**0.06**	**0.00**	**0.06**
	Cumulative N_{od}	**0.00**	**0.00**	**0.00**	**0.00**	**0.06**	**0.06**	
Toe	# of Moved Units	0	1	5	7	4	6	23
	# of Rocking Units	0	1	4	2	6	7	20
	$N_{od.\,t}$	**0.00**	**0.04**	**0.19**	**0.26**	**0.15**	**0.23**	**0.86**
	Cumulative $N_{od.\,t}$	**0.00**	**0.04**	**0.23**	**0.49**	**0.64**	**0.86**	

To optimize the cross-section, CS-B-5 was tested. In this test, the toe was moved farther from the armor layer to better placement of antifer blocks on the toe. Since the toe was protected by the armor layer in the prior experiment, the damage was increased. CS-B-5 was given at the prototype scale in Figure 5.11.

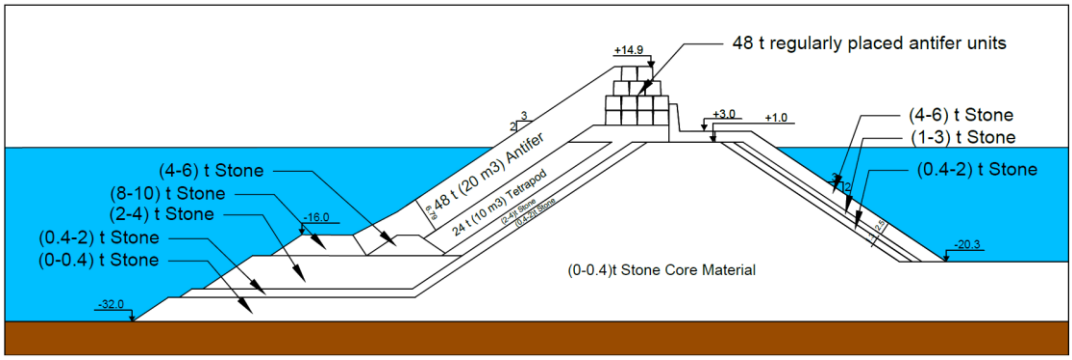

Figure 5.11: CS-B-5 in the prototype scale. (All dimensions given in the figure are in centimeters.)

Table 5.17 shows the cumulative damage amounts for each wave condition in N_{od}, depending on the number of displaced units for CS-B-5 and, the maximum N_{od} for armor layer and toe found as 0.40 and 1.24 respectively.

Table 5.17: Toe and armor layer damage measurements in CS-B-5

CS-B-5		Wave Set #						
		Set # 1						
		D1	D2	D3	D4-1	D4-2	D5	Σ
Armor Layer	# of Moved Units (Grey)	0	0	0	0	0	1	1
	# of Moved Units (Black)	0	0	0	0	0	1	1
	# of Moved Units (Green)	0	0	1	2	0	2	5
	# of Moved Units (Blue)	0	0	0	0	0	0	0
	# of Moved Units (Pink)	0	0	0	0	0	0	0
	# of Rocking Units	6	4	10	9	12	21	62
	N_{od}	**0.00**	**0.00**	**0.06**	**0.11**	**0.00**	**0.23**	**0.40**
	Cumulative N_{od}	**0.00**	**0.00**	**0.06**	**0.17**	**0.17**	**0.40**	
Toe	# of Moved Units	0	3	12	9	1	8	33
	# of Rocking Units	1	4	7	15	2	7	36
	$N_{od.\,t}$	**0.00**	**0.11**	**0.45**	**0.34**	**0.04**	**0.30**	**1.24**
	Cumulative $N_{od.\,t}$	**0.00**	**0.11**	**0.56**	**0.90**	**0.94**	**1.24**	

On the other hand, in the experiment of CS-B-6, in order to reduce the cost, 4-6 tons of stones, which is the heaviest stone group that can be supplied, have been tested in the toe. Since heavier stones have been damaged, to reduce toe damage, the toe upper elevation was lowered from 16 meters below the water level to 22.2 meters in the prototype. It was observed that toe damage was lessened. CS-B-6 was given at the prototype scale in Figure 5.12.

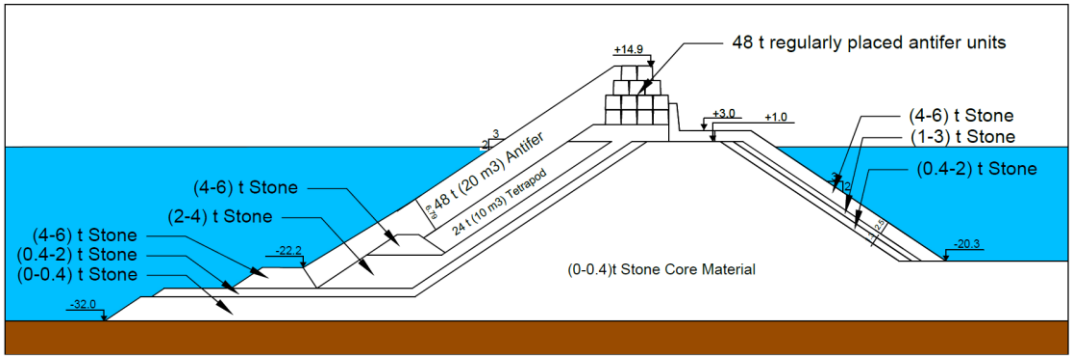

Figure 5.12: CS-B-6 in the prototype scale. (All dimensions given in the figure are in centimeters.)

Table 5.18 shows the cumulative damage amounts for each wave condition in N_{od}, depending on the number of displaced units for CS-B-6 and, the maximum N_{od} for armor layer and toe was found as 0.51 and 0.10 respectively. In addition, maximum

rear side damage S_{max} found as 0.3 and average rear side damage, S_{ave} for armor layer found as 0.1165.

Table 5.18: Toe and armor layer damage measurements in CS-B-6

CS-B-6		Wave Set #						
		Set # 1						
		D1	D2	D3	D4-1	D4-2	D5	Σ
Armor Layer	# of Moved Units (Grey)	0	0	2	1	0	2	5
	# of Moved Units (Black)	0	0	0	2	0	1	3
	# of Moved Units (Green)	0	0	0	0	0	0	0
	# of Moved Units (Blue)	0	0	0	1	0	0	1
	# of Moved Units (Pink)	0	0	0	0	0	0	0
	# of Rocking Units	9	13	12	3	1	21	59
	N_{od}	**0.00**	**0.00**	**0.11**	**0.23**	**0.00**	**0.17**	**0.51**
	Cumulative N_{od}	**0.00**	**0.00**	**0.11**	**0.34**	**0.34**	**0.51**	
Toe	# of Moved Units	0	0	1	1	1	1	4
	# of Rocking Units	0	2	0	3	5	0	10
	$N_{od.\,t}$	**0.00**	**0.00**	**0.03**	**0.03**	**0.03**	**0.03**	**0.10**
	Cumulative $N_{od.\,t}$	**0.00**	**0.00**	**0.03**	**0.05**	**0.08**	**0.10**	

In the experiment of CS-B-7, in order to reduce the damage to the armor layer, the water depth of the toe upper elevation in the prototype was increased to 19.9 meters. Although armor layer damage had decreased, damage in the toe had increased. CS-B-7 was given at the prototype scale in Figure 5.13.

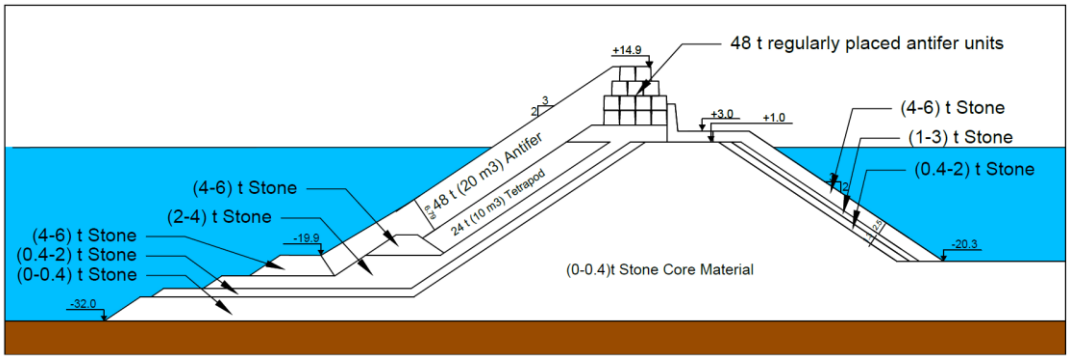

Figure 5.13: CS-B-7 in the prototype scale. (All dimensions given in the figure are in centimeters.)

Table 5.19 shows the cumulative damage amounts for each wave condition in N_{od}, depending on the number of displaced units for CS-B-7 and, the maximum N_{od} for armor layer and toe was found as 0.06 and 0.48 respectively. In addition, maximum

rear side damage S_{max} found as 2.5 and average rear side damage, S_{ave} for armor layer found as 0.4106

Table 5.19: Toe and armor layer damage measurements in CS-B-7

CS-B-7		Wave Set #						
		Set # 1						
		D1	D2	D3	D4-1	D4-2	D5	Σ
Armor Layer	# of Moved Units (Grey)	0	0	0	0	0	0	0
	# of Moved Units (Black)	0	0	0	0	1	0	1
	# of Moved Units (Green)	0	0	0	0	0	0	0
	# of Moved Units (Blue)	0	0	0	0	0	0	0
	# of Moved Units (Pink)	0	0	0	0	0	0	0
	# of Rocking Units	5	10	9	2	3	10	39
	N_{od}	**0.00**	**0.00**	**0.00**	**0.00**	**0.06**	**0.00**	**0.06**
	Cumulative N_{od}	**0.00**	**0.00**	**0.00**	**0.00**	**0.06**	**0.06**	
Toe	# of Moved Units	0	0	1	7	8	3	19
	# of Rocking Units	0	0	2	7	3	7	19
	$N_{od.\,t}$	**0.00**	**0.00**	**0.03**	**0.18**	**0.20**	**0.08**	**0.48**
	Cumulative $N_{od.\,t}$	**0.00**	**0.00**	**0.03**	**0.20**	**0.41**	**0.48**	

In the experiment of CS-B-8, it was decided to use 10 tons of cubes in the toe, considering both the difficulty in continuously supplying 4-6 tons of rock class and the reduction in toe and armor layer damage. The toe upper elevation has been raised to 16 meters below the water level in the prototype. It was observed that both toe and armor layer damage decreased. CS-B-8 was given at the prototype scale in Figure 5.14.

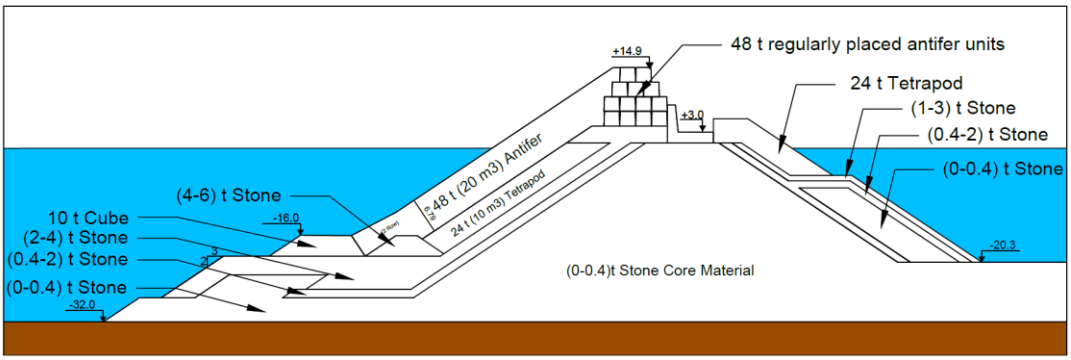

Figure 5.14: CS-B-8 in the prototype scale. (All dimensions given in the figure are in centimeters.)

In Table 5.20, measured wave overtopping values were given for each wave condition in the experiment CS-B-8 set two. The highest measured wave overtopping

was 119.97 liters. Corresponding wave overtopping discharge was 0.099 l/s/m at the model scale and 46 l/s/m at the prototype.

Table 5.20: Measured wave overtopping in CS-B-8 Set-2 (given in both model and prototype scale).

Set #			Wave Set # 2					
ALT. #		**Wave Condition**	**D1**	**D2**	**D3**	**D4-1**	**D4-2**	**D5**
		Water Level	W1	W2	W2	W1	W3	W3
		Exc./Oc. P.	*	**	***	****	****	*+
CS-B-8	Prototype Scale	**Wave Series Duration (hour)**	6.2	8.1	10.3	10.5	10.5	10.4
		Wave Overtopping. q (l/s/m)	**0.1**	**3.1**	**11**	**17.8**	**23.8**	**46**
	Model Scale	**Wave Overtopping Discharge, q (l/s/m)**	**0.0003**	**0.0068**	**0.0236**	**0.0383**	**0.0513**	**0.099**
		Wave Series Duration (hour)	6.2	8.1	10.3	10.5	10.5	10.4
		Wave Overtopping Discharge, q (l/s/m)	**0.1**	**3.1**	**11**	**17.8**	**23.8**	**46**
*:10 hrs., **:5 yr., ***: 50yr., ****:100 yr., *+: 100 yr., upper limit (90%); W1: LWL, W2: MWL, W3: HWL								

Table 5.21 shows the cumulative damage amounts for each wave condition in N_{od}, depending on the number of displaced units for CS-B-8 and, the maximum N_{od} for armor layer and toe was found as 0.06 and 0.18 respectively. Furthermore, maximum rear side damage S_{max} found as 0.6407 and average rear side damage, S_{ave} for armor layer found as 0.3521.

Table 5.21: Toe and armor layer damage in Set 1 and Set-2 of CS-B-8

CS-B-8		Wave Set #													
		Set # 1							Set # 2						
		D1	**D2**	**D3**	**D4-1**	**D4-2**	**D5**	**Σ**	**D1**	**D2**	**D3**	**D4-1**	**D4-2**	**D5**	**Σ**
Armor Layer	**# of Moved Units Grey)**	0	0	0	0	0	0	0	0	0	0	0	0	1	1
	# of Moved Units (Black)	0	0	0	0	0	0	0	0	0	0	0	0	0	0
	# of Moved Units Green)	0	0	0	0	0	0	0	0	0	0	0	0	0	0
	# of Moved Units (Blue)	0	0	0	0	0	0	0	0	0	0	0	0	0	0
	# of Moved Units (Pink)	0	0	0	0	0	0	0	0	0	0	0	0	0	0
	# of Rocking Units	8	12	9	5	8	16	58	7	22	16	9	2	7	63
	N_{od}	**0.00**	**0.00**	**0.00**	**0.00**	**0.00**	**0.00**	**0.00**	**0.00**	**0.00**	**0.00**	**0.00**	**0.00**	**0.06**	**0.06**
	Cumulative N_{od}	**0.00**	**0.00**	**0.00**	**0.00**	**0.00**	**0.00**		**0.00**	**0.00**	**0.00**	**0.00**	**0.00**	**0.06**	
Toe	**# of Moved Units**	0	0	2	1	2	0	5	0	2	2	2	0	1	7
	# of Rocking Units	3	4	3	2	4	2	18	1	4	2	3	1	1	12
	$N_{od.\ t}$	**0.00**	**0.00**	**0.05**	**0.03**	**0.05**	**0.00**	**0.13**	**0.00**	**0.05**	**0.05**	**0.05**	**0.00**	**0.03**	**0.18**
	Cumulative $N_{od.\ t}$	**0.00**	**0.00**	**0.05**	**0.08**	**0.13**	**0.13**		**0.00**	**0.05**	**0.10**	**0.15**	**0.15**	**0.18**	

Table 5.22 shows the summary of the measured rear side damage level for each alternative cross-section.

Table 5.22: The amount of rear side damage measured in Set-1 and Set-2 of each experiment for CS-B.

Cross-Section/ Damage Level	S_{max}	S_{ave}
CS-B-1	10.277	6.027
CS-B-2	6.314	2.478
CS-B-3	-	-
CS-B-4	0.894	0.396
CS-B-5	-	-
CS-B-6	0.302	0.117
CS-B-7	2.541	0.411
CS-B-8	-	-

For CS-B-3, the test was done to find a solution to the specific problem mentioned above and for CS-B-5, since just the toe was moved away a little from the armor layer, the rear side damage measurement was not done. Furthermore, For CS-B-8, on the rear side, since tetrapod is used, which is an artificial unit, the damage would not be defined by using the *S* parameter.

The summary of seaward armor layer damage results is shown in Table 5.23.

Table 5.23: Summary of damage results

Set #			Wave Set # 1							Wave Set # 2						
ALT.	W. Cond.		D1	D2	D3	D4-1	D4-2	D5	Σ	D1	D2	D3	D4-1	D4-2	D5	Σ
	Wat. Le.		W1	W2	W2	W1	W3	W3		W1	W2	W2	W1	W3	W3	
	Exc./Oc. P.		*	**	***	****	****	*+		*	**	***	****	****	*+	
CS-B-1	A. L.	N_{od}	0.06	0.28	0.79	0.62	0.11	0.23	**2.09**	0.17	0.23	0.85	0.28	0.28	0.11	**1.92**
		Σ	0.06	0.34	1.13	1.75	1.86	2.09		0.17	0.40	1.24	1.53	1.81	1.92	
	Toe	$N_{od.t}$	0.03	0.41	0.28	0.74	0.28	0.15	**1.89**	0.03	0.26	1.15	1.05	0.48	0.38	**3.34**
		Σ	0.03	0.43	0.71	1.45	1.73	1.89		0.03	0.28	1.43	2.47	2.96	3.34	
CS-B-2	A. L.	N_{od}	0.11	0.23	0.45	0.17	0.06	0.00	**1.02**	-	-	-	-	-	-	**-**
		Σ	0.11	0.34	0.79	0.96	1.02	1.02		-	-	-	-	-	-	
	Toe	$N_{od.t}$	0.00	0.28	0.83	0.52	0.35	0.55	**2.52**	-	-	-	-	-	-	**-**
		Σ	0.00	0.28	1.11	1.62	1.97	2.52		-	-	-	-	-	-	
CS-B-3	A. L.	N_{od}	-	-	-	0.11	0.06	0.11	**0.28**	-	-	-	-	-	-	**-**
		Σ	-	-	-	0.11	0.17	0.28		-	-	-	-	-	-	
	Toe	$N_{od.t}$	-	-	-	0.86	0.17	0.07	**1.11**	-	-	-	-	-	-	**-**
		Σ	-	-	-	0.86	1.04	1.11		-	-	-	-	-	-	
CS-B-4	A. L.	N_{od}	0.00	0.00	0.00	0.00	0.06	0.00	**0.06**	-	-	-	-	-	-	**-**
		Σ	0.00	0.00	0.00	0.00	0.06	0.06		-	-	-	-	-	-	
	Toe	$N_{od.t}$	0.00	0.04	0.19	0.26	0.15	0.23	**0.86**	-	-	-	-	-	-	**-**
		Σ	0.00	0.04	0.23	0.49	0.64	0.86		-	-	-	-	-	-	
CS-B-5	A. L.	N_{od}	0.00	0.00	0.06	0.11	0.00	0.23	**0.40**	-	-	-	-	-	-	**-**
		Σ	0.00	0.00	0.06	0.17	0.17	0.40		-	-	-	-	-	-	
	Toe	$N_{od.t}$	0.00	0.11	0.45	0.34	0.04	0.30	**1.24**	-	-	-	-	-	-	**-**
		Σ	0.00	0.11	0.56	0.90	0.94	1.24		-	-	-	-	-	-	
CS-B-6	A. L.	N_{od}	0.00	0.00	0.11	0.23	0.00	0.17	**0.51**	-	-	-	-	-	-	**-**
		Σ	0.00	0.00	0.11	0.34	0.34	0.51		-	-	-	-	-	-	
	Toe	$N_{od.t}$	0.00	0.00	0.03	0.03	0.03	0.03	**0.10**	-	-	-	-	-	-	**-**
		Σ	0.00	0.00	0.03	0.05	0.08	0.10		-	-	-	-	-	-	
CS-B-7	A. L.	N_{od}	0.00	0.00	0.00	0.00	0.06	0.00	**0.06**	-	-	-	-	-	-	**-**
		Σ	0.00	0.00	0.00	0.00	0.06	0.06		-	-	-	-	-	-	
	Toe	$N_{od.t}$	0.00	0.00	0.03	0.18	0.20	0.08	**0.48**	-	-	-	-	-	-	**-**
		Σ	0.00	0.00	0.03	0.20	0.41	0.48		-	-	-	-	-	-	
CS-B-8	A. L.	N_{od}	0.00	0.00	0.00	0.00	0.00	0.00	**0.00**	0.00	0.00	0.00	0.00	0.00	0.06	**0.06**
		Σ	0.00	0.00	0.00	0.00	0.00	0.00		0.00	0.00	0.00	0.00	0.00	0.06	
	Toe	$N_{od.t}$	0.00	0.00	0.05	0.03	0.05	0.00	**0.13**	0.00	0.05	0.05	0.05	0.00	0.03	**0.18**
		Σ	0.00	0.00	0.05	0.08	0.13	0.13		0.00	0.05	0.10	0.15	0.15	0.18	

*:10 hrs., **:5 yr., ***: 50yr., ****:100 yr., *+: 100 yr., upper limit (90%); W1: LWL, W2: MWL, W3: HWL

In Figure 5.15, all tested cross-sections for CS-B are shown focusing on the main difference (toe) between each alternative. This figure is given as a summary of all the modifications in CS-B described above.

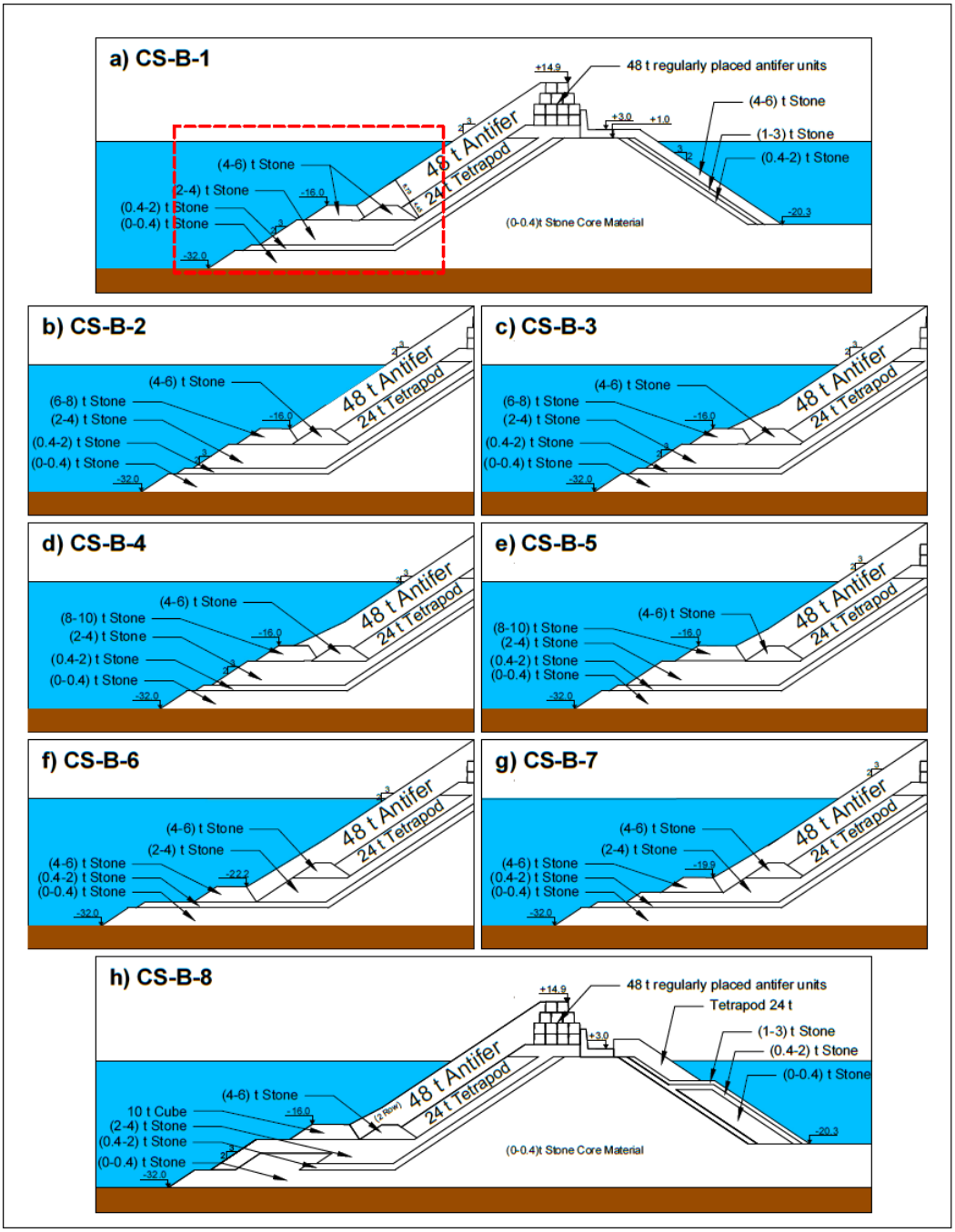

Figure 5.15: All tested cross-sections for CS-B at prototype scale (All dimensions given in the figure are in meters).

CHAPTER 6

DISCUSSION OF RESULTS

In this chapter, the results of the experiments are discussed in aspects of the stability of the toe, armor, crest, and rear-side and wave overtopping. It is noted that the existing breakwater cross-sections has not been experimentally tested in this study as the existing breakwater cross-sections were already damaged significantly or failed in prototype scale. Therefore, it is expected that these cross-sections would fail in laboratory experiments.

6.1 Armor layer stability

Through observation of the experiments, there was no major problem regarding the interaction between antifer units placed on top of tetrapod units. However, as there was not a typical filter layer forming smooth surfaces beneath the antifer layer, placement of antifer units was found moderately harder in the model. Thus, it is highly possible to have difficulty in the placement of antifer blocks on the construction site. In the Figure 6.1, examples of photos showing the placement of antifer units on the tetrapod units are given.

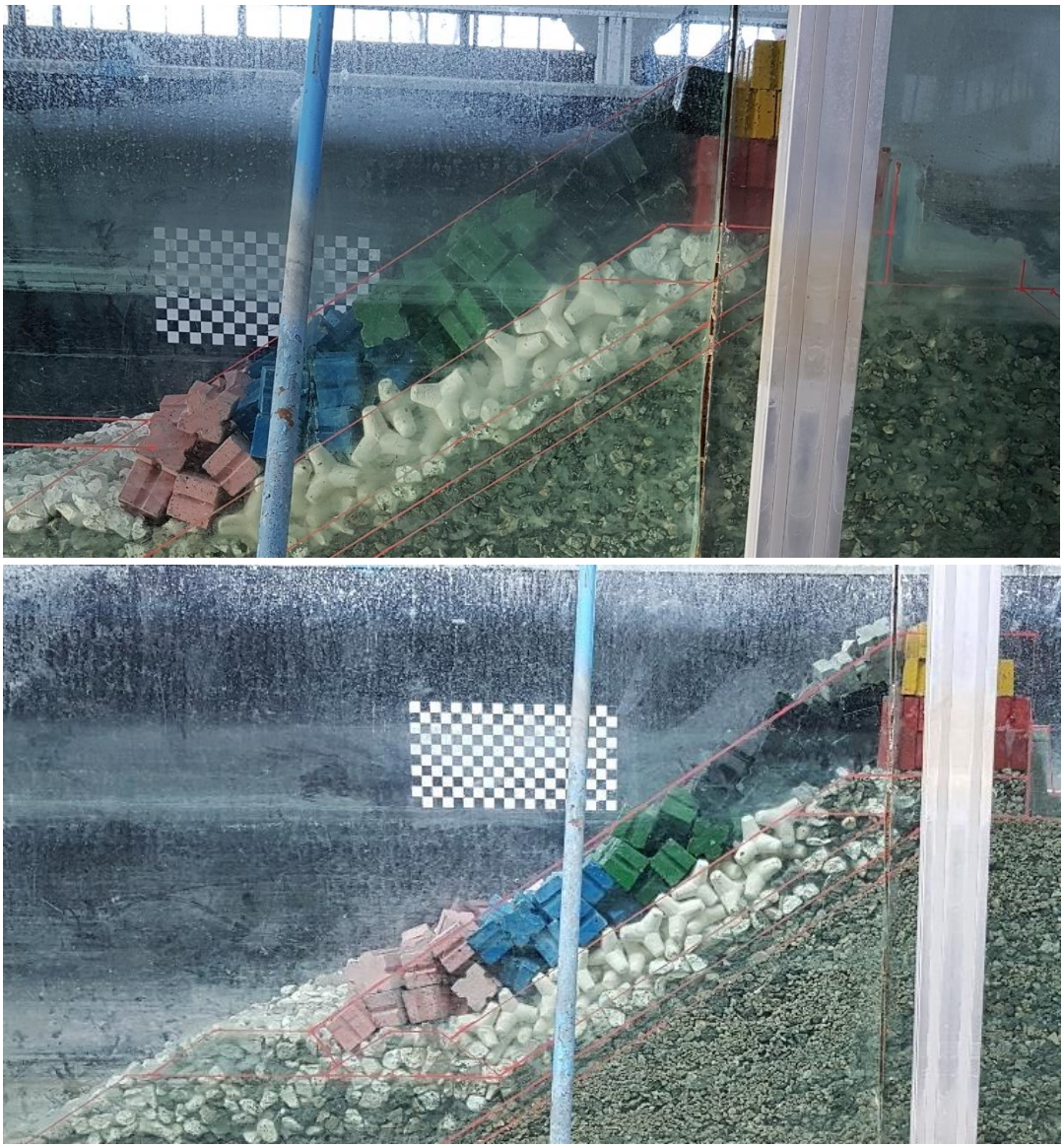

Figure 6.1: Example photos of studied cross-sections (the upper one is from CS-A, the bottom one is from CS-B)

Furthermore, for the armor layer, two different placement methods were used. On the slope of the armor layer, an irregular placement of antifer units with a packing density of 0.61 (Frens, 2007) was used. At the crest, antifers are placed regularly where the bottom sides are down. In the Figure 6.2, photos from the top view and rear side of the cross-section showing regularly placed antifer blocks on the crest are given.

Figure 6.2: Regularly placed antifer units on the crest

These regularly placed antifer units acted as crown wall and helped irregularly placed antifer units to stand firm without falling behind. However, these regular units do not form a rigid structure. By observation, none of the regularly placed antifer fell on top of the crown wall or further away. Furthermore, even after overload wave conditions, the top of regularly placed antifer units did not move by more than half a Dn_{50} of an antifer block. Nevertheless, one should note that those, whose movement was observed are likely to have a free space in front of them (which could be expressed as those who are not protected by irregularly placed antifer units). Thus, in the construction site, this is one of the circumstances that should be carefully observed and considered.

6.2 Toe stability of cross-sections

The first toe design of CS-A has approximately initial level damage with 42-ton cubes in the shallower section, however, considering the cost of operation, manufacturing, and transportation, the toe layer stone size changed to lighter natural stones. After reducing the upper elevation of the toe and the stone size of the toe, wave overtopping increased as expected. From CS-A-1 to CS-A-3, maximum wave overtopping increases as the upper elevation of the toe decrease. But, from CS-A-3 to CS-A-4, the upper elevation of the toe increase. Thus, maximum wave overtopping decreased.

In the first design, heavier stone size (42-ton cubes) with a less upper elevation was used in the toe. Thus, the damage in the toe layer is less than in the last two cross-sections. Although the upper elevation of the toe increased, the damage in the toe increased since lighter natural stones were used in CS-A-3 and CS-A-4. However, this damage could be defined as moderate damage. Therefore, after any significant storm event, the breakwater should be investigated to look for damage, and maintenance should be done for the toe layer. Also, an increase in wave overtopping could result in serious damage and endanger lives, during the storm event, the port operations should be temporarily stopped.

In the deeper section (Section 2-2), to decrease the toe damage, natural stone size was increased through the experiment. Although damage in the toe layer has been calculated as moderate damage in CS-B-5, CS-B-6 was applied to find a cheaper solution and was taken into account for procurement of quarry stones, which has a lighter stone size in the toe layer and deeper upper elevation of the toe layer. However, the damage in the armor layer increased. Thus, CS-B-7 is implemented. In this case, toe layer damage increased. Hence, CS-B-8 was tested with the same upper elevation of the toe layer as CS-B-5. To further decrease the damage in the toe layer, 8–10 tons of natural stones were replaced with 10-ton cubes.

Furthermore, an incompatibility was found between existing and new designs in CS-B-2 shown in Figure 6.3. It could be expressed as follows. Since in the armor layer irregularly placed antifer units are used, their placement line is not a smooth surface. At the start of the slope on the toe, antifer units are not placed in two layers to follow the slope line. A part of the existing toe takes up space from the new antifer armor layer region. Thus, in the experiments carried out, more armor layer damage occurred than expected in the areas where the antifer blocks were not in two rows (on the toe).

Figure 6.3: The incompatibility between existing and new designs

6.3 Overtopping comparison

The overtopping discharges measured in the experiments were compared to two different artificial neural networks (ANNs), recommended by EurOtop (2018), which predict the mean overtopping discharges at various types of coastal structures. These ANNs are EurOtop ANN and EurOtop-database (Formentin et al., 2017; Zanuttigh et al., 2016; EurOtop, 2018), and CLASH ANN database (Van Gent et al., 2007). For simplicity, the CLASH ANN database will be called CLASH, EurOtop ANN, and EurOtop-database will be called EurOtop in the rest of this section.

Four criteria given in EurOtop (2018) should be mentioned before the description of the computations. It might be necessary to correct for scale and model effect, where overtopping rates are less than 1.0 l/s per meter. In this study, mostly, overtopping discharges exceed 1.0 l/s per meter except for the D1 wave condition. Therefore, no correction is needed. EurOtop (2018) also mentioned that in a model, to minimize scale effects of surface tension, water depths should be much greater than h = 2.0 cm, wave periods larger than T = 0.35 s, and wave heights greater than H_s = 5.0 cm. In this study, these conditions are satisfied. In addition, the width of the gutter plate or any device measuring wave overtopping should be typically greater than 20 armor units. In this study, it is approximately 15 armor units. Thus, some scale effects could be observed; however, this scale effect is assumed to be minor as there are still many armor units along the gutter. Finally, it was mentioned that considering the stability of the armor layer, the Reynolds number should exceed $Re_{crit} = 3 * 10^4$ for rubble mound breakwaters. In this study, this criterion is satisfied.

To represent the effect of the regularly placed antifer units on the crest and packing density of irregularly placed antifers along the armor layer on the wave overtopping discharges, the roughness coefficient was changed in the ANN computations. Three roughness coefficient values were selected since, in the EurOtop manual, the roughness coefficient of two-layer antifer units is 0.50 and shown as $\gamma_{f,E}$. The limit values of antifer units given in CLASH are 0.47 & 0.65, so 0.50 roughness

coefficient could be used for both ANN estimations. For each alternative, wave overtopping values obtained from the ANN computations and measured wave overtopping values will be given in more detail in Appendix A.

First of all, input variables should be defined for ANN calculations. In Table 6.1, common input parameters for both CLASH and EurOtop are given. However, since they have other concerns regarding geometrical features, their unique input parameters are shown separately. In the table, the definition of the parameter, its symbol, and its units are shown.

Table 6.1:Input parameter definition and units for ANN (adapted from EurOtop, 2018)

	Definition of the parameter	**Input**	**Units**
Common	Label/ID of the test	Name	[-]
	Water depth at the toe of the structure	h	[m]
	Significant wave height at the toe of the structure	$H_{m0,t}$	[m]
	Spectral wave period at the toe of the structure	$T_{m-1,0,t}$	[s]
	Wave obliquity	β	[°]
	Toe submergence	h_t	[m]
	Toe width	B_t	[m]
	Berm submergence	h_b	[m]
	Horizontal berm width	B	[m]
	Cotangent of the angle that the part of the structure below the berm makes with a horizontal	$cot\alpha_d$	[-]
	Cotangent of the angle that the part of the structure above the berm makes with a horizontal	$cot\alpha_u$	[-]
	Roughness factor for cotαd	$\gamma_{f,d}$	[-]
	Roughness factor for cotαu	$\gamma_{f,u}$	[-]
	Armor crest height with respect to SWL	A_c	[m]
	Crest height with respect to SWL	R_c	[m]
	Crest width	G_c	[m]
	Berm slope	$\tan\alpha_B$	[-]
EurOtop	Size of the structure elements along cotαd	D_d	[m]
	Size of the structure elements along cotαu	D_u	[m]
	Cotangent of the foreshore slope; 1000 = horizontal foreshore	m	[-]

Since the measured overtopping discharges were compared to two different artificial neural networks, this part of the study, firstly, examines these ANN individually. After that results will be compared with both ANNs outputs.

EurOtop

To have a better understanding of EurOtop input parameters, a simple sketch showing input variables is given in Figure 6.4.

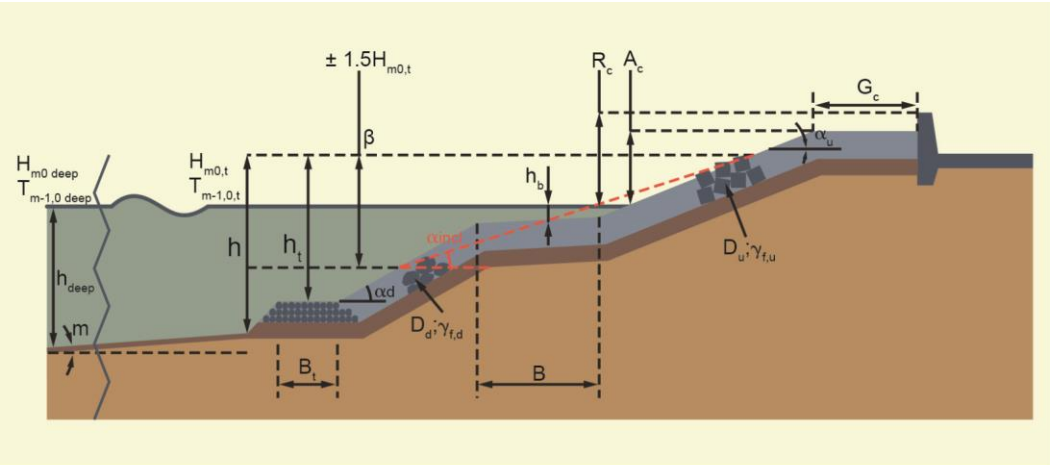

Figure 6.4: A sketch of input parameter definition for EurOtop (adopted from EurOtop, 2018)

In Table 6.2, sample input values of EurOtop in the case of CS-B-8 in the case of one roughness coefficient ($\gamma_{f,E}$ = 0.50) are given. In the below table, all values are dependent on cross-section geometry and change with each wave condition except for significant wave height at the toe of the structure spectral wave period at the toe of the structure, and wave obliquity.

Table 6.2: Sample input values of EurOtop for CS-B

Test ID	D-1	D-2	D-3	D4-1	D4-2	D5
m	1000	1000	1000	1000	1000	1000
h	0.535	0.536	0.537	0.535	0.549	0.549
$H_{m0,t}$	0.09	0.115	0.135	0.143	0.143	0.153
$T_{m-1,0,t}$	1.25	1.33	1.45	1.49	1.49	1.55
β	0	0	0	0	0	0
h_t	0.162	0.163	0.164	0.162	0.176	0.176
B_t	0.156	0.156	0.156	0.156	0.156	0.156
h_b	0	0	0	0	0	0
B	0	0	0	0	0	0
$cot(\alpha_d)$	1.5	1.5	1.5	1.5	1.5	1.5
$cot(\alpha_u)$	1.5	1.5	1.5	1.5	1.5	1.5
$\gamma_{f,d}$	0.5	0.5	0.5	0.5	0.5	0.5
$\gamma_{f,u}$	0.5	0.5	0.5	0.5	0.5	0.5
D_d	0.0452	0.0452	0.0452	0.0452	0.0452	0.0452
D_u	0.0452	0.0452	0.0452	0.0452	0.0452	0.0452
A_c	0.246	0.245	0.244	0.246	0.232	0.232
R_c	0.131	0.13	0.129	0.131	0.117	0.117
G_c	0.167	0.167	0.167	0.167	0.167	0.167

Nearly all input parameters entered in CLASH for overtopping discharge calculation are the same as those entered in EurOtop However, they have some unique entries. In the case of EurOtop, these are the cotangent of the foreshore slope (m) and the size of the structure elements along the cotangent of the angle that the part of the structure below and above the berm makes with a horizontal (D_d and D_u). EurOtop includes more data for training and prediction than CLASH. EurOtop also gives additional parameters for K_r and K_t, which have narrower confidence bands and smaller dispersion. In comparison to the CLASH, the EurOtop has larger confidence intervals and a more pronounced bias.

CLASH

To visualize input parameters, a simple sketch showing input variables is given in Figure 6.5.

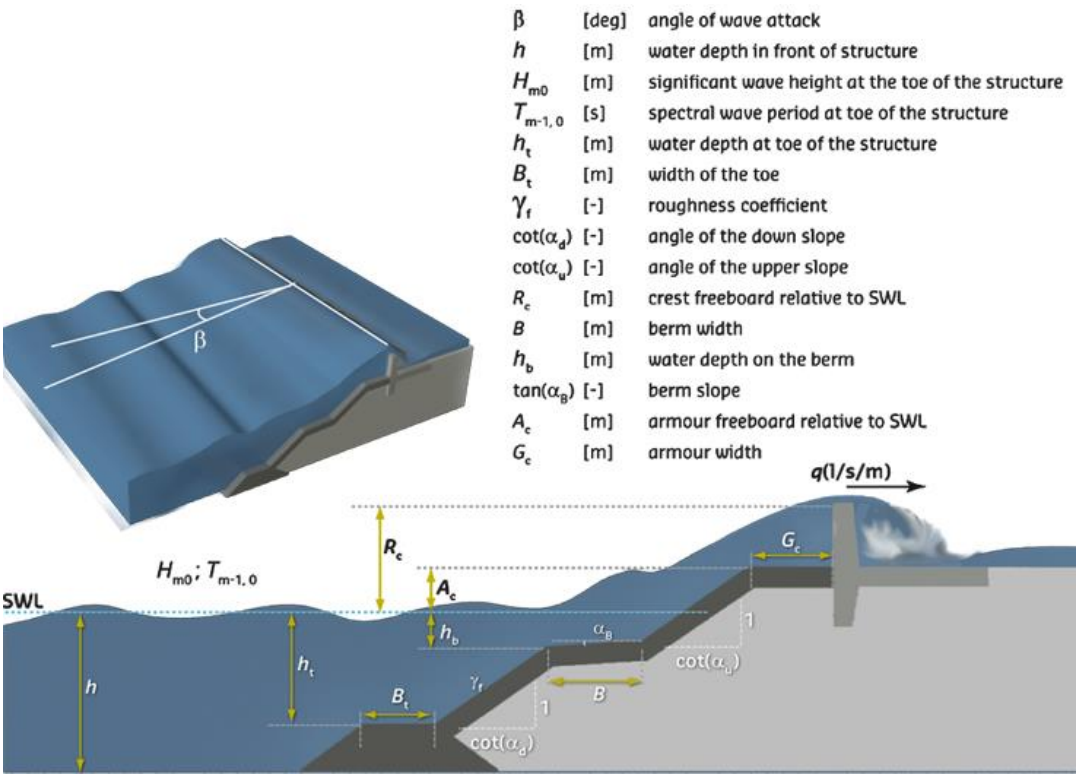

Figure 6.5: A sketch of input parameter definition for CLASH (adopted from van Gent et al., 2007)

In Table 6.3, a sample input values of CLASH in the case of CS-B-8 in the case of one roughness coefficient ($\gamma_{f,E}$ = 0.50) are given. In the below table, all values are dependent on cross-section geometry and change with each wave condition except for significant wave height at the toe of the structure spectral wave period at the toe of the structure, and wave obliquity. One of the different variables from EurOtop is the tangent of the berm slope, which is also dependent on the geometry of the cross-section.

Table 6.3: Sample input values of CLASH for CS-B

Scenario	D1	D2	D3	D4-1	D4-2	D5
β	0	0	0	0	0	0
h	0.535	0.536	0.537	0.535	0.549	0.549
H_{m0}	0.09	0.115	0.135	0.143	0.143	0.153
$T_{m-1.0}$	1.25	1.33	1.45	1.49	1.49	1.55
h_t	0.162	0.163	0.164	0.162	0.176	0.176
B_t	0.1563	0.1563	0.1563	0.1563	0.1563	0.1563
γ_f	0.50	0.50	0.50	0.50	0.50	0.50
$\cot\alpha_d$	1.5	1.5	1.5	1.5	1.5	1.5
$\cot\alpha_u$	1.5	1.5	1.5	1.5	1.5	1.5
R_c	0.131	0.13	0.129	0.131	0.117	0.117
B	0	0	0	0	0	0
h_b	0	0	0	0	0	0
$\tan\alpha_B$	0	0	0	0	0	0
A_c	0.246	0.245	0.244	0.246	0.232	0.232
G_c	0.1667	0.1667	0.1667	0.1667	0.1667	0.1667

So far, the input variables of both ANNs are examined briefly. For each wave condition, these geometric features will remain the same, however, an increase or decrease in water level changes the input values. The main focus is to explain differences between this complex cross-section and traditional cross-sections such as regular placement of antifer units on the crest and using two different artificial units on the armor layer or not, by changing the roughness coefficient value.

Figure 6.6 shows measured overtopping discharges, CLASH, and EurOtop estimations for each wave condition in CS-A. For overtopping comparison figures in this part of the study, the red cross sign shows measured overtopping discharges. The blue line shows estimated overtopping discharges from CLASH having roughness coefficients of $\gamma_{f,E}$ =0.50, whereas blue dotted line shows estimated overtopping discharges from EurOtop having a roughness coefficient of $\gamma_{f,E}$ =0.50.

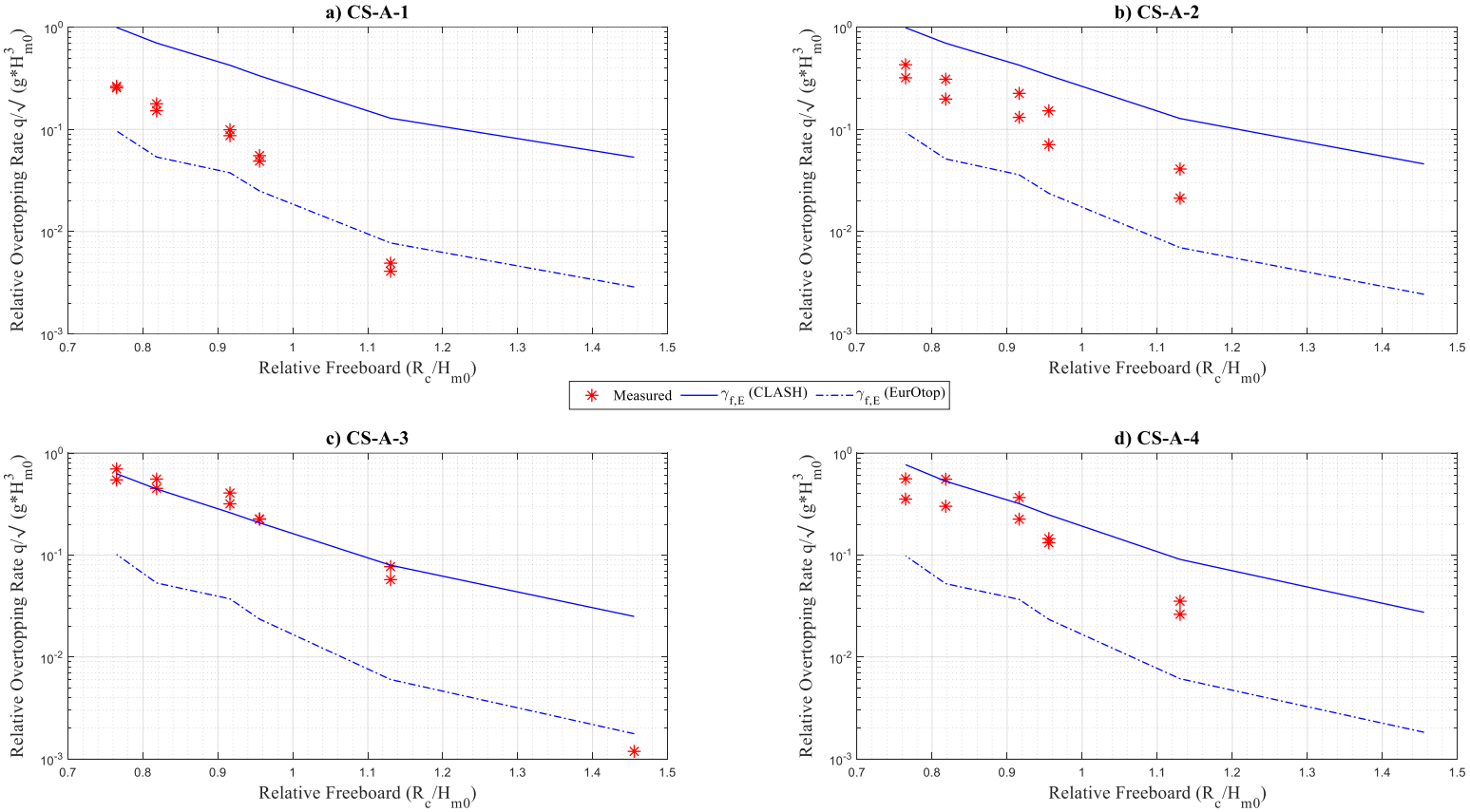

Figure 6.6: Overtopping comparison with ANN and CS-A measured values

In Figure 6.6a for CS-A-1, measured values wander between the estimated overtopping discharges from CLASH having a roughness coefficient of $\gamma_{f,E}$ = 0.50 and EurOtop estimation having a roughness coefficient of $\gamma_{f,E}$ = 0.50, closer to EurOtop estimation. However, the measured value during the D2 wave condition is less than all estimations. The reason for this could be that measured D2 data (0.3 l/s per m in prototype) is less than 1.0 l/s per m in the prototype. Thus, there could be a need for correction for scale and model effects, and the discharges under this limit can be computed wrong using the ANNs by its nature (EurOtop, 2018).

In Figure 6.6b for CS-A-2, measured overtopping discharges vary between again both ANN estimations.

In Figure 6.6c for CS-A-3, all measured data fitted well with the estimated data from EurOtop having a roughness coefficient ($\gamma_{f,E} = 0.50$) except for the D1 wave condition. The data measured for the D1 wave condition is nearly equal to 0.0 l/s per m in the prototype. Therefore, there is a need for correction since the data could have calculation issues with ANN, as stated above based on the notes given in EurOtop, 2018.

In Figure 6.6d for CS-A-4, the measured data wanders around estimated data having a roughness coefficient of $\gamma_{f,E} = 0.50$ from CLASH and EurOtop, closer to CLASH estimations.

Figure 6.7 shows measured overtopping discharges, CLASH, and EurOtop estimations for each wave condition in CS-B-8.

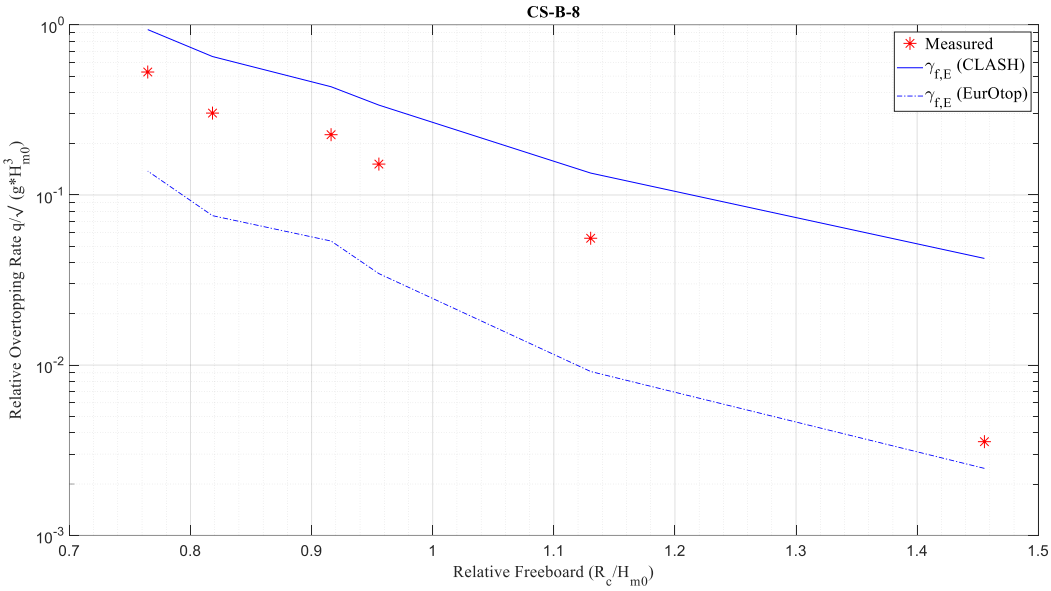

Figure 6.7: Overtopping comparison with ANN and CS-B measured values

In Figure 6.7, the measured data wanders between CLASH and EurOtop estimations, closer to CLASH estimation except for the D1 wave condition. The data measured for the D1 wave condition is equal to 0.1 l/s per m in the prototype. Therefore, there is a need for correction since the data could have calculation issues with ANN, as stated above based on the notes given in EurOtop, 2018.

To sum it up, the overtopping discharges obtained from EurOtop mostly underestimate measured overtopping values for the selected roughness coefficient ($\gamma_{f,E}$ = 0.50), whereas CLASH generally overestimates measured overtopping values. Moreover, the measured wave overtopping discharges is in between the range of CLASH estimation having a roughness coefficient of $\gamma_{f,E}$ = 0.50 and EurOtop estimation having a roughness coefficient of $\gamma_{f,E}$ = 0.50.

To be able to explain these results, one should examine cross-section geometries. When comparing CS-A-2 and CS-A-1, a noticeable change is that the upper elevation of the toe layer is decreased from 9.6 meters to 8.2 meters under the SWL.

Furthermore, when comparing CS-A-3 and CS-A-4, again noticeable change is the upper elevation of the toe is increased from 14.0 meters to 13.7 meters below the SWL. For both case comparisons, measured overtopping data approaches to the EurOtop estimation, having roughness coefficient value of $\gamma_{f,E}$ = 0.50. (see Figure 6.6a and Figure 6.6b & Figure 6.6d and Figure 6.6c).

Moreover, one can pay attention to toe width changes. When the toe width increased from 19.7 meters to 23.2 meters (CS-A-2 to CS-A-1) and 4.0 meters to 8.0 meters (CS-A-3 to CS-A-4), measured overtopping data approaches EurOtop estimation.

Another reason for these differences can be the usage of different armor units (rock vs cubes) at the toe. However, it is very hard to compare the cross-sections having different units at the toe (CS-A-1 and CS-A-2 with CS-A-3 and CS-A-4), as the geometries of these cross-sections are far more different.

Overall, the above observations imply that all measured data varies between both ANN estimations. It should be noted that these observations are limited as the number of experiments is limited and the cross-sections have significant geometrical differences preventing controlled experiments. However, the results still present insights into the potential physical explanations, especially indicating the importance of the placement patterns of the armor units in the overtopping performances of these breakwaters.

6.4 Rear side stability

Damage to the rubble mound breakwater armor layer is measured by considering the eroded area around the water level. However, in cases where artificial concrete blocks are used in the armor layer, it is recommended to define damage in terms of displaced blocks instead of making damage profile measurements (Van der Meer, 2017). For this reason, in the present study, the damage caused by wave overtopping

discharge on the rear side of the breakwater is expressed with the S parameter. The damage in the breakwater armor layer is given in terms of N_{od}.

In Table 5.22, $\boldsymbol{S_{max}}$ and $\boldsymbol{S_{ave}}$ were given for each alternative in CS-B. For CS-B-3 and CS-B-5, laser measurements were not done. Furthermore, since in CS-B-8, tetrapod units (artificial units) were used, the damage could not be calculated by using the S parameter. However, through the observations, no damage was observed except for the rocking artificial units. In Table 6.4, rear side, armor, and toe layer damage, the upper elevation of toe layer, and toe width are given.

Table 6.4: Rear side damage comparison

Case	Armor Layer Damage (N_{od})	Toe Layer Damage (N_{od})	Rear Side Damage (S_{ave})	Upper Elevation of Toe Layer (m)	Toe Width (m)
CS-B-1	2.09	1.89	6.0	-16.0	7.5
CS-B-2	1.02	2.52	2.5	-16.0	7.5
CS-B-4	0.06	0.86	0.4	-16.0	3.8
CS-B-6	0.51	0.10	0.1	-22.2	7.5
CS-B-7	0.06	0.48	0.4	-19.9	7.5

For each alternative, the damage on the rear side decreased. However, in the case of CS-B-7, the damage increased. Therefore, to ensure the safety of the rear side, the weight of stones used for the rear side should be increased. Considering the tetrapod removal process and tetrapod weight, which is the necessity of the new design, it was decided to put tetrapods at the rear side armor layer in CS-B-8. These tetrapod units, which are removed from the seaward side to enable the application of a new armor layer, were placed behind the existing crown wall above the still water level to approximately 0.6 H_s (5 meters) below the still water level in the prototype.

In the experiments, the rear side damage decreases until the CS-B-7. The upper elevation of the toe is the same from CS-B-1 to CS-B-5. Therefore, the only change is the stone weight in the toe layer except for CS-B-5, in which the toe layer was

shifted to the seaside and thus, rear-side damage would not be measured. From CS-B-1 to CS-B-4, both armor layer damage and toe layer damage decreased. The reason for this could be the stability of the toe layer. Since the toe layer is more stable than the previous cross-sections, it has functioned better. Thus, the wave effect on the armor layer was also decreased. Hence, the stability of the armor layer increased and rear side damage decreases.

Moreover, when comparing CS-B-1 and CS-B-2, even though the damage of the toe layer increases, the armor layer damage decreases by half. Thus, it can be expected that the armor layer could dissipate wave energy more than the toe layer can. In the case of CS-B-2 and CS-B-4 comparison, both toe and armor layer damage decrease. Thus, wave energy dissipates more, and less rear-side damage occurred as expected. When the upper elevation of the toe decreases, one expects higher wave overtopping. However, in the case of CS-B-6, less rear-side damage is calculated. The reason for this could be damage to both the toe and armor layer decreased. The more wave energy is transferred to the rear side as wave overtopping.

Furthermore, from CS-B-6 to CS-B-7 rear side damage increases although the upper elevation of the toe layer increases. However, when examining toe layer damage, it increases. Thus, this could result in a decrease in the efficiency of wave energy dissipation. Also, when comparing CS-B-4 and CS-B-7, although the upper elevation of the toe layer decreased, which could result in more wave overtopping, rear side damage remained the same. The reason for this could be a decrease in toe layer damage. Since in CS-B-4, with a greater upper elevation toe layer, the toe is damaged more. Thus, wave overtopping affects the rear side more than it is supposed to.

The most important factor affecting rear side damage is wave overtopping. As one can know, one of the toe functions is decreasing wave energy transferring as wave overtopping. Therefore, the wave overtopping decreases when damage in the toe layer decreases. Hence, rear-side damage also decreases. So, toe layer-related changes could affect the rear side damage.

CHAPTER 7

CONCLUSION

In this study, the aim is to reinforce an existing breakwater consisting of tetrapod units with antifer blocks. Experiments were done in two sections. These are the shallower section (CS-A: Section 4-4) and the deeper section (CS-B: Section 2-2). The stability of the new armor layer, the stability of the new toe design and its optimization, the effects of changing the placement of the armor layer on the crest to regular placement, and overtopping discharge and its effects on the stability of the rear side armor layer are the main subjects of this study.

The first concern is regarding the interaction between antifer units and tetrapod units on the stability. In the physical model experiments, no negative effects were observed on stability caused by the interaction of tetrapod and antifer units. The placement of antifers over tetrapods or the stone filter layer did not differ much. It has been observed that the damages that occurred under the wave set and water level conditions (Table 4.4) in the armor layer strengthened with 48 tons of antifer artificial block units meet the design criteria and the cross-sectional stability is achieved.

For CS-A, although the first designed toe with 42 tons cubes had nearly the initial level of damage and less overtopping discharges, considering the economy and conveyor belt system at the rear side placed on a piled quay, 4-6 ton stones with an approximately medium level of damage are decided to use. However, as expected, not to have much damage, the upper elevation of the toe descended from 8.2 meters to 13.7 meters below the still water level. In the case of the deeper section (Section 2-2), the first design is toe weight is 4-6 tons stones but, the damage level was found as not acceptable. Therefore, heavier units are used.

For CS-B, as mentioned in Section 6.2, an incompatibility has been found. To be able to solve this problem, the new toe is moved away from the existing toe, and the slope of the armor layer changes when it is close to the toe layer. Also, since one layer as an armor layer could lead to excessive damage, it is recommended to place and control two- rows of antifer blocks during the construction phase. Furthermore, increasing the toe upper elevation results in toe damage, and increasing stone weight in the toe could result in either shortage of needed stone class or using a lot heavier stones, which is more costly, 10 cubes are used in the toe layer considering crane capacity and procurement of the 4-6 tons of stones.

Another finding is that by changing the irregular placement of antifer blocks into regular placement on the crest, one can form a part that functions similarly to a crown wall. Although in this part some movement of antifer blocks has been observed, mostly, rocking or movement less than D_{n50} in D5 wave condition (significant wave height with a 100-year recurrence period corresponding to the overload condition in the high-water level). So, this part functions as a crown wall and is stabilized. However, one remark should be done about the protection from the armor layer of this part. These movements could be seen on the antifers, which are not protected from the seaward side. Also, this region decreases the cost by eliminating the need for an improved crown wall. It has been observed that these antifer blocks placed regularly on the crest reduce the overtopping discharges.

The important outcome of these experiments is that measured overtopping wave discharges vary compared to between both ANN estimations. In fact, the measured overtopping values for the range of the roughness coefficient are largely understated by the overtopping discharges obtained from EurOtop. On the other hand, computed overtopping discharges from CLASH using a roughness coefficient in the range of $\gamma_{f,E} = 0.50$ overestimate the overtopping measurements for several cases (see e.g.

CS-A-1, CS-A-2 and CS-B-8) and has a good agreement with several cases (see e.g. CS-A-3), as shown in Figure 6.6 and Figure 6.7.

Therefore, we recommend using CLASH ANN with $\gamma_{f,E} = 0.50$ to be on the safe side for the design of reinforced structures similar to the cross-sections presented in this study.

It has been observed that the wave overtopping discharges remained at the safe level for people, vehicles, and structures behind the harbor (rear side) in the D1 wave condition for all alternatives. In other wave conditions, it was suggested to stop the port operations and it was stated that the port structures behind the breakwater could be damaged.

The damage on the rear side is measured by a laser meter and by measuring overtopping discharges, the suitability of usage for the rear side operation of the breakwater is investigated. For the shallower section (Section 4-4), the damage did not measure by a laser meter since in that region there is a conveyor system in the prototype. The damage is calculated by using the *S* parameter.

An important future remark is that since potential (or already done by the storm events) damage to tetrapods during antifer settlement was not taken into account in the experiments, one could investigate the effects of breakage of tetrapod units on the stability and overtopping discharges. For future works, it would be nice to examine the relationship between rear side damage, armor layer and toe layer damage, and wave overtopping with a more detailed and controlled set of experiments.

REFERENCES

Arıkan, G. (2010). *Reliability-based design model for rubble-mound coastal defense structures* [Ph.D. - Doctoral Program]. Middle East Technical University.

ASCE Port Sines Investigation Panel, Edge, B. L., Fairweather, V., Baird, W. F., Magoon, O. T., Caldwell, J. M., & Treadwell, D. D. (1982). Failure of the breakwater at the port Sines, Portugal. the American Society of Civil Engineers 345 East 47th Street New York, New York 10017.

Baird, W. F., Caldwell, J. M., Edge, B. L., Magoon, O. T., & Treadwell, D. D. (1980). Report on the damages to the Sines Breakwater, Portugal. *Coastal Engineering Proceedings*, (17), 181-181.

Burcharth, H. F., d'Angremond, K., Van der Meer, J. W., & Liu, Z. (2000). Empirical formula for breakage of dolosse and tetrapods. *Coastal Engineering*, *40*(3), 183-206. https://doi.org/10.1016/S0378-3839(00)00010-7

Burcharth, H. F., Liu, Z., & Troch, P. (1999). Scaling of core material in rubble mound breakwater model tests. In *Fifth International Conference on Coastal and Port Engineering in Developing Countries: Proceedings of the COPEDEC V: Cape Town, South Africa, 19-23 April, 1999* (pp. 1518-1528). COPEDEC.

Burcharth, H. F. (1987). *The Lessons From Recent Breakwater Failures: developments in breakwater design.* Paper presented at Technical Congress On Inshore Engineering, Vancouver, Canada.

Domingo, A. M. V. (2012). *Evaluation of concrete armour units used to repair damaged dolos breakwaters*. *June*, 152.

Eldrup, M. R., Lykke Andersen, T., & Burcharth, H. F. (2019). Stability of rubble mound breakwaters—A study of the notional permeability factor, based on physical model tests. *Water*, *11*(5), 934. https://doi.org/10.3390/w11050934

EurOtop. 2018. *Manual on wave overtopping of sea defences and related structures. An overtopping manual largely based on European research, but worldwide application. 2nd ed*. http://www.overtopping-manual.com.

Frens, A. B. (2007). *The impact of placement method on Antifer-block stability*. *May*, 146.

Formentin S.M., Zanuttigh B. and Van der Meer J.W., 2017. A Neural Network TOOL for predicting wave reflection, overtopping and transmission, Coastal Engineering Journal, 59, No. 2 (2017), 1750006, 31 pp.

Goda, Y. (2010). Random seas and design of maritime structures, second edition.

World Scientific Publishing Company.

Guler, H. G., Kirezci, Ç., Baykal, C., Tarakcıoğlu, G. Ö., Işık, E., Ergin, A., Yalçıner, A. C., & Guler, I. (2022). Major Damage At A Port Located In The Southwestern Black Sea Region Due To A Severe Storm. (*in preparation*).

Gunbak, A. R., Ergin, A. (1985). Damage and repair of Antalya Harbor Breakwater. *In Design and Construction of Mounds for Breakwaters and Coastal Protection, ed: Per Bruun*, Elsevier.

Günbak, A. R. (1999). Antifer cubes on rubble mound breakwaters. *Proceedings of the COPEDEC, Cape Town, South Africa*.

Hudson, R. Y., Hermann, F. A., Sager, R. A., Whalin, R. W., Keulegan, G. H., Chatham, C. E., and Hales, L. Z. (1979). "Coastal Hydraulic Models" Special Report No.5, US Army Engineer Waterways Experiment Station, Vicksburg, Missisippi.

Hughes, S. A. (1993). *Physical Models and Laboratory Techniques in Coastal Engineering*. https://doi.org/10.1142/2154

Hydralab. (2007). *Guidelines for physical model testing of breakwaters : Rubble mound breakwaters*. *August*, 1–39.

Kılıçoğlu, A., Aral, F. & Yalçıner, A. C. (2004). Expert report on Giresun Port, Ankara, Turkey.

Ligteringen, H. (1987). Breakwater Engineering. *Interdisciplinary Science Reviews*, *12*(1), 41-55. https://doi.org/10.1179/isr.1987.12.1.41

Maddrell, R. (2005). Lessons re-learnt from the failure of marine structures. In *International Conference on Coastlines, structures, and breakwaters 2005* (pp. 139-152). Thomas Telford Publishing.

Magoon, O. T., Sloan, R. L. & Foote, G. L. (1974). Damages to coastal structures. *Proceedings of the Fourteenth Coastal Engineering Conference, Copenhagen, Denmark*, Vol 3., Ch. 97, ASCE, pp. 1665-1676.

Mansard, E. P. D., & Funke, E. R. (1980). The measurement of incident and reflected spectra using a least squares method. *Coastal Engineering 1980*, 154–172. https://doi.org/10.1061/9780872622647.008

Markle, D. G. (1982). *Kahului Breakwater Stability Study, Kahului, Maui, Hawaii. Hydraulic Model Investigation*. ARMY ENGINEER WATERWAYS EXPERIMENT STATION VICKSBURG MS HYDRAULICS LAB.

METU. (2020). "Zonguldak Eren Limanı Kıyı Yapıları Güçlendirme ve Liman İçi Çalkantı İyileştirme Araştırma Projesi Ara Raporu" METU, Department of

Civil Engineering, Coastal And Ocean Engineering Research Center, Ankara, Turkey, 2020.

METU. (2022). “Zonguldak Eren Limanı Kıyı Yapıları Güçlendirme ve Liman İçi Çalkantı İyileştirme Araştırma Projesi Final Raporu” METU, Department of Civil Engineering, Coastal And Ocean Engineering Research Center, Ankara, Turkey, 2020.

Muttray, M., & Reedijk, B. (2009). Design of concrete armor layers. *Hansa International Maritime Journal*, *6*, 111-118.

U S Army Corps Of Engineers, N. (2002). Coastal Engineering Manual. *Coastal Engineering Manual*, *August 2001*, 1–62.

Van der Meer, J. W. (1999, June). Design of concrete armor layers. In *Proceedings of the Coastal Structures* (Vol. 99, pp. 213-221).

Van der Meer, J. W. (2017). Application and stability criteria for rock and artificial units. Dikes and Revetments: Design, Maintenance and Safety Assessment.

Van Gent, M.R.A., H.F.P. van den Boogaard, B. Pozueta and J.R. Medina (2007), Neural network modelling of wave overtopping at coastal structures, Elsevier, Coastal Engineering, Vol.54, pp. 586-593.”

Sargent, F. E., Markle, D. G., & Grace, P. J. (1988). Case histories of Corps breakwater and jetty structures. *US Army Corps of Engineers, Washington, DC. Report No.: Technical Report REMR-CO-3*.

SWAN (2019). User's Manual. Delft University of Technology, Environmental Fluid Mechanics Section, http://swan.sourceforge.net (Version 41.31).

Wiegel, R. L. (1982). Breakwater damage by severe storm waves and tsunami waves. *Report.* Berkeley, California.

Yagci, O., & Kapdasli, S. (2003). Alternative placement technique for antifer blocks used on breakwaters. *Ocean Engineering*, *30*(11), 1433–1451. https://doi.org/10.1016/S0029-8018(02)00134-8

Zanuttigh B., Formentin S.M., and Van der Meer J.W., 2016. Prediction of extreme and tolerable wave overtopping discharges through an advanced neural network, Ocean Engineering, 127, 7-22.

APPENDICES

A. Overtopping comparison

In the below tables, wave overtopping discharge estimations from CLASH and EurOtop given for roughness coefficient of 0.50 ($\gamma_{f,E}$), and measured wave overtopping discharges for each wave condition are given.

CS-A-1

Table 7.1:ANN & measured wave overtopping comparison for CS-A-1

Database	CLASH	EurOtop	Measured	
Wave Condition	$\gamma_{f,E}$	$\gamma_{f,E}$	Set-1	Set-2
D1	0.0045	0.0002	0.0000	0.0000
D2	0.0157	0.0009	0.0005	0.0006
D3	0.0519	0.0039	0.0076	0.0086
D4-1	0.0718	0.0064	0.0147	0.0168
D4-2	0.1185	0.0091	0.0258	0.0301
D5	0.1864	0.0181	0.0495	0.0478

CS-A-2

Table 7.2: ANN & measured wave overtopping comparison for CS-A-2

Database	CLASH	EurOtop	Measured	
Wave Condition	$\gamma_{f,E}$	$\gamma_{f,E}$	Set-1	Set-2
D1	0.0039	0.0002	0.0000	0.0000
D2	0.0156	0.0009	0.005	0.0026
D3	0.0523	0.0037	0.0236	0.011
D4-1	0.0720	0.0061	0.0381	0.0222
D4-2	0.1180	0.0087	0.0524	0.0335
D5	0.1850	0.0175	0.0804	0.0599

CS-A-3

Table 7.3: ANN & measured wave overtopping comparison for CS-A-3

Database	CLASH	EurOtop	Measured	
Wave Condition	$\gamma_{f,E}$	$\gamma_{f,E}$	Set-1	Set-2
D1	0.0021	0.0001	0.0001	0.0000
D2	0.0097	0.0007	0.0094	0.007
D3	0.0322	0.0037	0.0349	0.0351
D4-1	0.0441	0.0063	0.0538	0.0687
D4-2	0.0752	0.0090	0.0763	0.0941
D5	0.1177	0.0190	0.1023	0.131

CS-A-4

Table 7.4: ANN & measured wave overtopping comparison for CS-A-4

Database	CLASH	EurOtop	Measured	
Wave Condition	$\gamma_{f,E}$	$\gamma_{f,E}$	Set-1	Set-2
D1	0.0023	0.0002	0.0000	0.0000
D2	0.0111	0.0007	0.0032	0.0043
D3	0.0385	0.0036	0.0205	0.0225
D4-1	0.0541	0.0062	0.0381	0.0621
D4-2	0.0897	0.0089	0.051	0.0939
D5	0.1443	0.0184	0.0663	0.1048

CS-B-8

Table 7.5: ANN & measured wave overtopping comparison for CS-B-8

Database	CLASH	EurOtop	Measured
Wave Condition	$\gamma_{f,E}$	$\gamma_{f,E}$	Set-2
D1	0.0036	0.0002	0.0003
D2	0.0164	0.0010	0.0068
D3	0.0524	0.0051	0.0236
D4-1	0.0733	0.0088	0.0383
D4-2	0.1103	0.0123	0.0513
D5	0.1758	0.0253	0.099